LAWRENCE
LIVERMORE
NATIONAL
LABORATORY

UCRL-CONF-219628

Structures in Molecular Clouds: Modeling

J. O. Kane, D. D. Ryutov, B. A. Remington, M. Pound, A. Mizuta

March 8, 2006

Structures in #Molecular Clouds: Modeling
Houston, TX, United States
March 11, 2006 through March 14, 2006

Updated October 14, 2003

Structures in Molecular Clouds: Modeling

Jave Kane, Dmitri Ryutov, Bruce Remington
Lawrence Livermore National Laboratory

Marc Pound, University of Maryland

Akira Mizuta, Max Planck Institute für Astrophysik, Garching

This work was performed under the auspices of the U.S. DOE by UC, LLNL under Contract W-7405-Eng-48.

Theory and modeling of molecular cloud structures has a long history

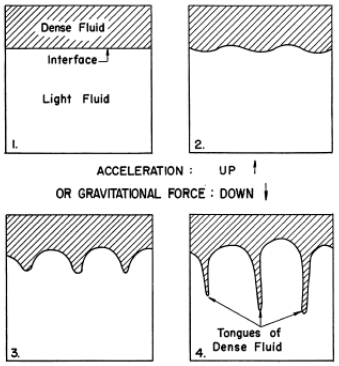

FIG. 5.—Development of Rayleigh-Taylor instability

M16 — RT
Spitzer, ApJ **120**, 1 (1954)
Frieman, ApJ **120**, 18 (1954)

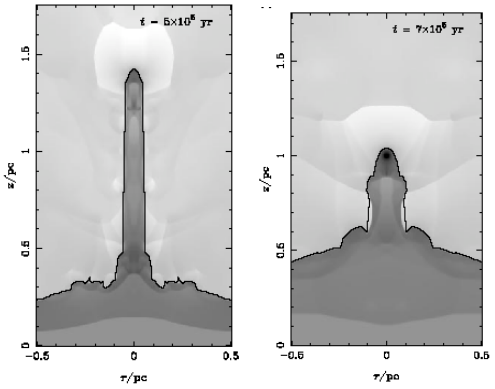

M16
Williams, Ward-Thompson & Whitworth,
Mon. Not R. Astron. Soc. **327**, 788 (2001)

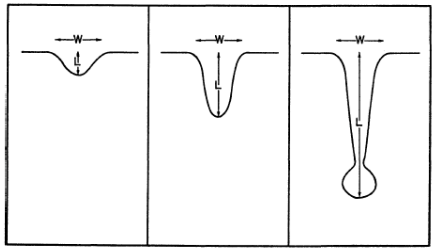

FIG. 3.—Schematic evolution of a comet-tail structure Three stages, time increasing from left to right.

Comets
Osterbrock, ApJ **125**, 6220 (1957)

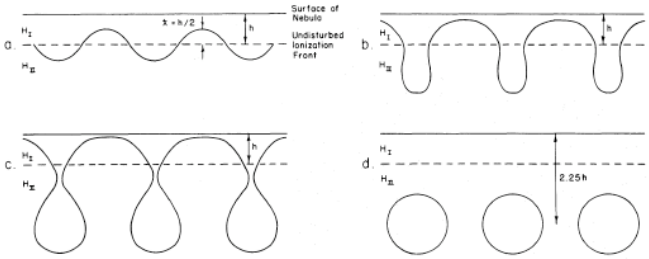

Helix Nebula
Capriotti, ApJ **179**, 495 (1973)

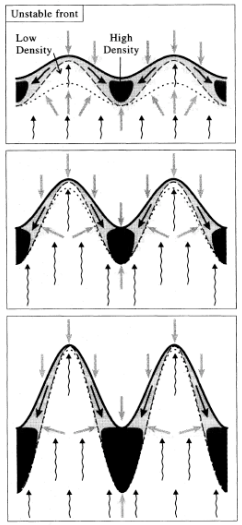

García-Segura and Franco,
ApJ **469,** 171 (1996)

Hydrodynamics, instability of ionization fronts
Kahn, Rev. Mod. Phys. **30**, 1058 (1958)
Vandervoort, ApJ **135,** 212 (1962)
Axford, ApJ **140,** 112 (1964)
Arons & Max, ApJ **196,** L77 (1975)
Reipurth, A&A **117** (1983)
Bertoldi, ApJ **346**, 735 (1989)
Bertoldi & McKee, ApJ **354**, 529 (1990)
Williams, MNRAS **331**, 693 (2002)
Lefloch & Lazareff, A&A **289**, 559 (1994);
A&A **301**, 522 (1995)

Protestellar disks, AMR
Richling & Yorke ,A&A **327**, 317 (1997)
Yorke & Kaisig, Comp. Phys. Comm., 89, 29 (1995)

Cooling
Neufeld *et al.*, ApJS **100,** 132 (1995)

Magnetic fields and turbulence
Ostriker, Gammie, & Stone, ApJ **513,** 259 (1999);
ApJ **546,** 980 (2001).

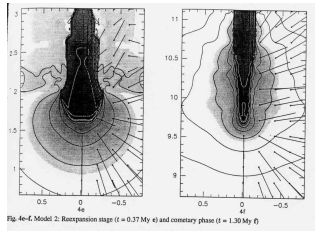

Comets — RDI
Lefloch & Lazareff, A&A **289**, 559 (1994);

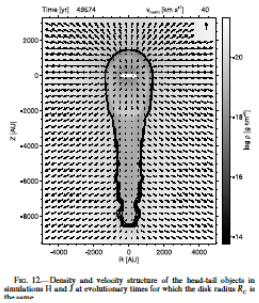

Protostellar disks
Richling & Yorke ApJ **539**, 258 (2000)

How do we make pillars in the laboratory?

Target Chamber of Nova laser

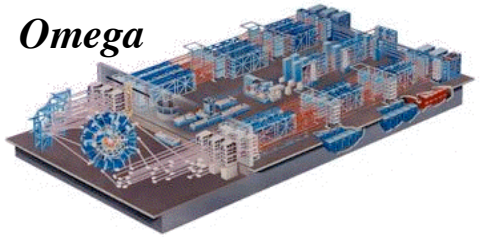

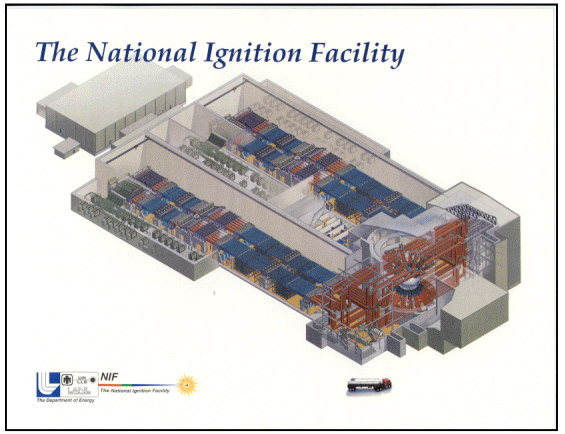

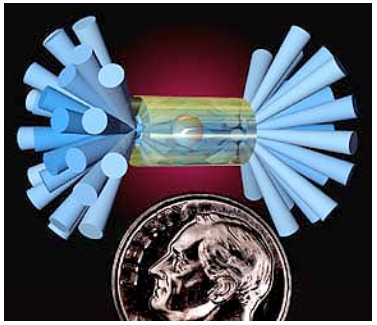

Radiation cavity
(hohlraum)

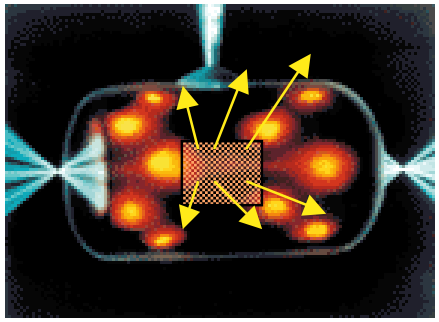

We are planning laser experiments to test models of formation of the Pillars — prototypes exist

1) Prototypical Rayleigh-Taylor experiment

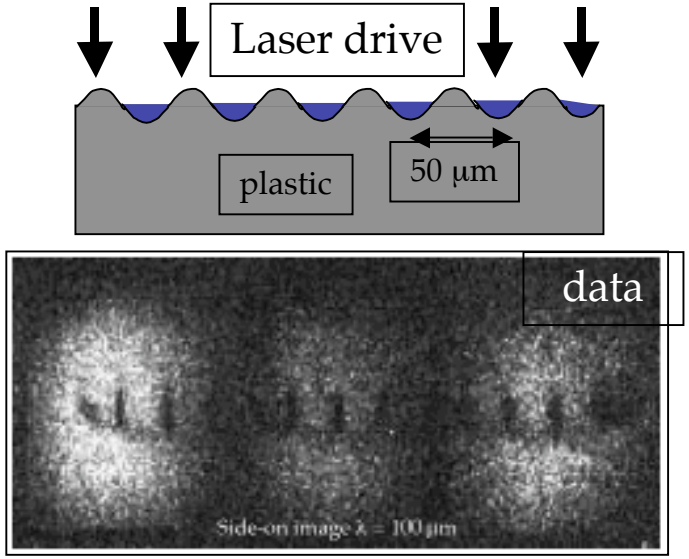

Remington, B. A. 1992, *et al.*, Phys. Fluids B **4**, 967

2) Prototypical Cometary experiment

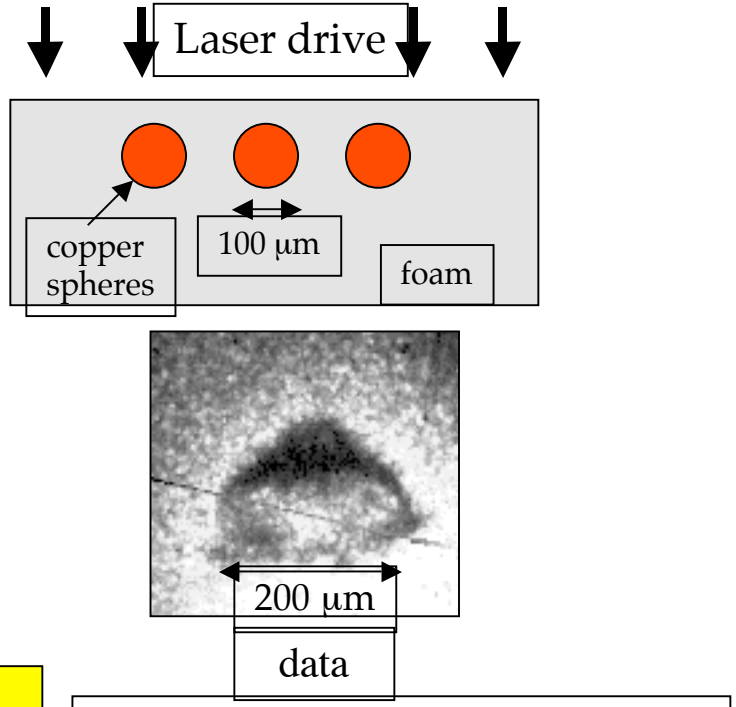

Klein, R. I., *et al*. 2000, ApJS **127**, 379
Robey, H. F. *et al.* , submitted to PRL (2001)

We can test both the RT and cometary models experimentally

We first considered a compressible Rayleigh Taylor (RT) model

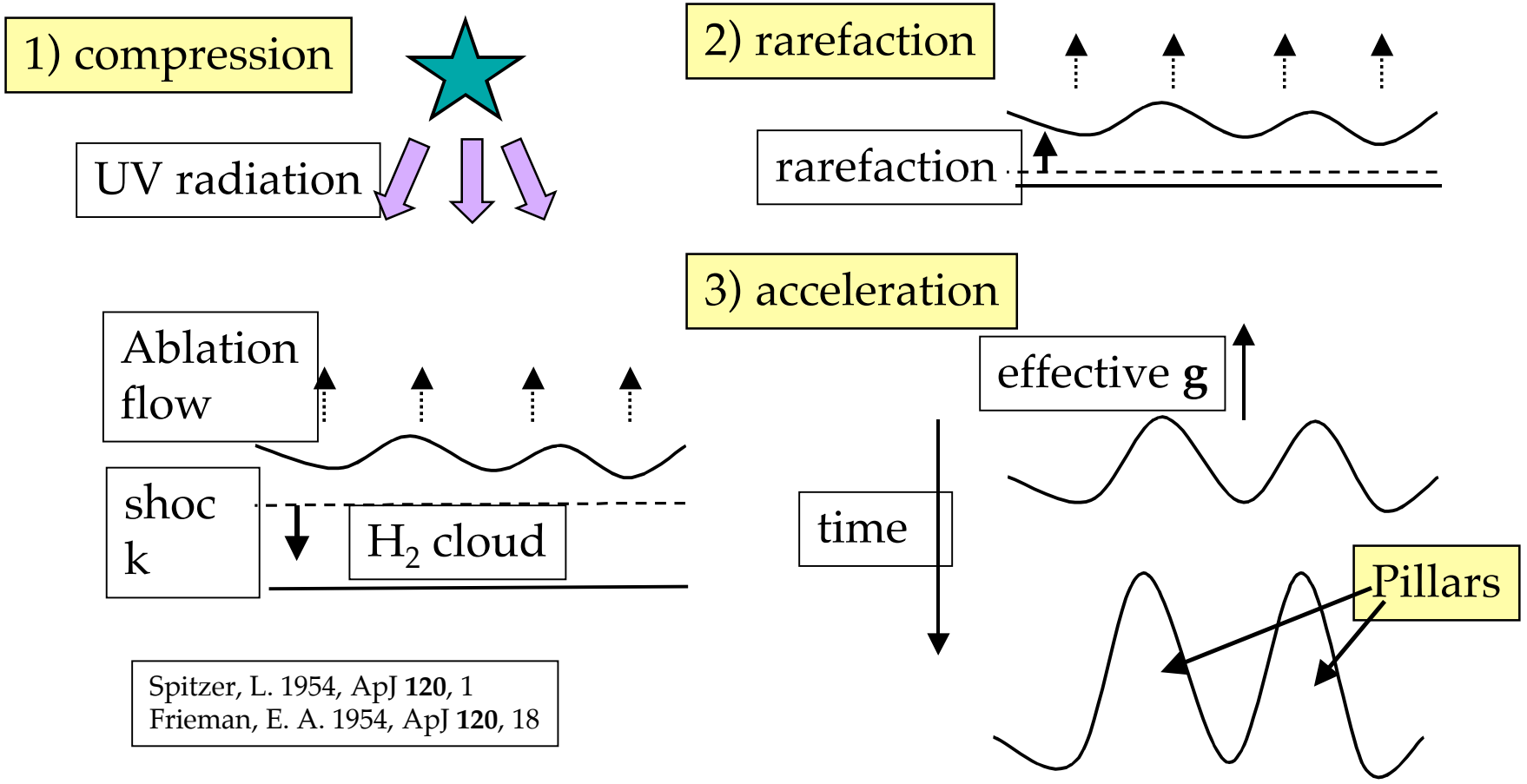

Spitzer, L. 1954, ApJ **120**, 1
Frieman, E. A. 1954, ApJ **120**, 18

The basic equations describe the hydrodynamics, absorption and re-emission of radiation, and EOS

Hydrodynamics

$$\frac{\partial \rho}{\partial t} + \nabla \cdot (\rho \boldsymbol{u}) = 0,$$

$$\frac{\partial (\rho \boldsymbol{u})}{\partial t} + \nabla \cdot (\rho \boldsymbol{u}\boldsymbol{u} + \boldsymbol{P}) = 0,$$

$$\frac{\partial}{\partial t}\left(\rho\left(\frac{1}{2}\boldsymbol{u}^2 + \epsilon\right)\right) + \nabla \cdot \left(\left(\rho\left(\frac{1}{2}\boldsymbol{u}^2 + \epsilon\right) + p\right)\boldsymbol{u}\right) = -q_{re} + q_{uv} - q_{mol},$$

Mizuta *et al.*,ApJ **621**, 803–807, (2005)

$$q_{re} = (nf)^2 \beta_B k_B T,$$

$$q_{uv} = W n a (1-f) J,$$

$$q_{mol} = n_{mol}^2 \times 10^{-29} \mathrm{erg\ cm^{-3} s^{-1}},$$

$$T = \frac{m_p}{k_b}\frac{4\epsilon}{7f+5},$$

$$n_{mol} = n(1-f)/2.$$

$$n\frac{\partial f}{\partial t} + n\boldsymbol{u} \cdot \nabla f = an(1-f)J - \alpha_B n^2 f^2,$$

Recombination

Absorption

$$\frac{\partial J}{\partial y} = -an(1-f)J,$$

EOS

$$p = \underbrace{\frac{2(3f+1)}{7f+5}\rho\epsilon}_{\text{thermal p.}} + \underbrace{p_M\left(\frac{\rho}{\rho_M}\right)^{\gamma_M}}_{\text{magnetic p.}}.$$

a: photoionization cross-section, α_B =case B recombination coefficient

J: incident photon flux, f =n_i/n: ionization degree, γ_M=4/3 (f=0 --> grad(J)=max, f=1 --> grad(J)=0)

Cooling and magnetic fields may matter

- The Eagle Nebula is thought to be transparent to the radiation in the millimeter and sub-millimeter range (in part, because of strong sheared flows).
- The relevant cooling functions were obtained in: D.A. Neufeld and M.J. Kaufman, ApJ, **418**, 263 (1993) and D.A. Neufeld, S. Lepp, G.J. Melnik, ApJ Supplement, **100**, 132 (1995)
- There exists a significant uncertainty in applying these results to the Eagle Nebula, caused by uncertainties in the composition and ionization degree.
- Still, most probably, the cooling time is much shorter than the hydrodynamic time, meaning that the shocked material cools down to its initial temperature ~40 K at a short distance behind the shock front.
- This would mean that the gas behind the shock would be compressed to the density two orders of magnitude higher than evaluated by M. Pound.
- As is well known, this paradox can potentially be resolved by introducing the magnetic field.

A random magnetic field may restore ordinary hydrodynamics with an effective adiabatic index

- In order to make the magnetic pressure an important player in the pressure balance, one has to have the magnetic pressure in the shocked material to be~ the ablation pressure, $B^2/8\pi \sim p_{abl}$. The latter, according to M. Pound, is $\sim 1.3 \cdot 10^8$ erg/cm^3, yielding the required magnetic field strength, B~600 μG
- The pre-shocked magnetic field can be 1.5 – 2 times weaker, depending of the adiabat (we mean here the adiabat relating the magnetic pressure and the plasma pressure, not the gaseous pressure, which is small because of strong radiation)
- For a random magnetic field, the adiabat index is 4/3; for a regular magnetic field parallel to the shock front it is 2, yielding the density compression rate of 7 and 3, respectively.
- If the magnetic field is random, the overall hydrodynamics does not differ significantly from the case where the pressure is simply a gas pressure. For the regular magnetic field, the anisotropic nature of the magnetic stress tensor may introduce some new physics

Ryutov et al., Proc. 5th Conf. HEDLA, AIP **703**, 415 (2004).
Ostriker, Gammie, & Stone, ApJ **513,** 259 (1999); ApJ **546,** 980 (2001).

We wrote a code with Van Leer hydro, simple ray tracing, and simple models for opacity and absorption

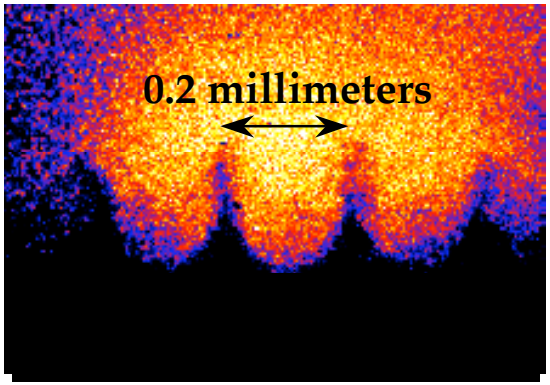

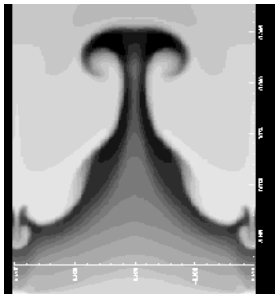

PROMETHEUS New code

Kane J *et al*., ApJ 478, L75 (1997);
Remington B A *et al*. Phys. Plasmas 4 (1994)

Opacity

$\kappa = f(T)\,(n/n_0)\,\kappa_0$

$f(T) = 1,\ T < T_0$

$\exp\{[(T-T_0)/(A_T T_0)^2]\},\ T \geq T_0$

$T_0 = 200$ K, $A_T = 200$, $n_0 = 5 \times 10^4$ /cm^3,

$\kappa_0 = 100$ / <width of cloud>

1) Evaporated material has low opacity

2) Cloud absorbs in thin surface layer

Energy deposition

$\Delta F = F \times \exp(-\kappa\, dx)$

$u \rightarrow u + \Delta F/dx\, dt\ /\ \rho$

$F \rightarrow F - \Delta F$

3) Directed radiation is absorbed as specified by above opacity

Equation of State

Ideal gas $\gamma = 5/3$

4) We could vary EOS to model

- isothermal (rapidly cooling) cloud
- turbulent magnetic pressure

The compressible model produces results consistent with measured velocity and column density

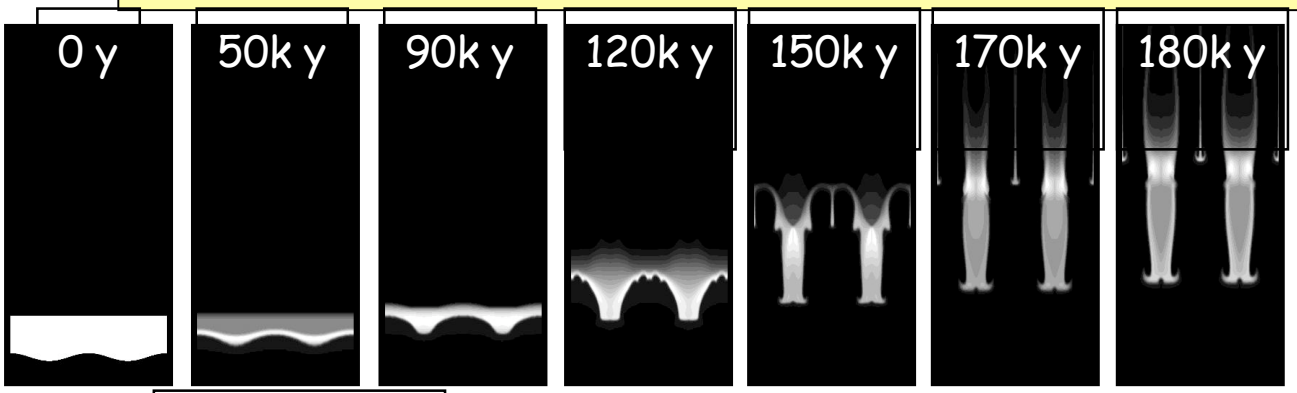

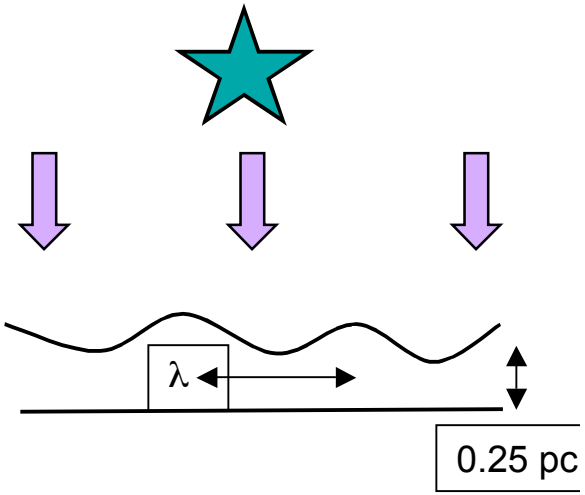

compression

acceleration

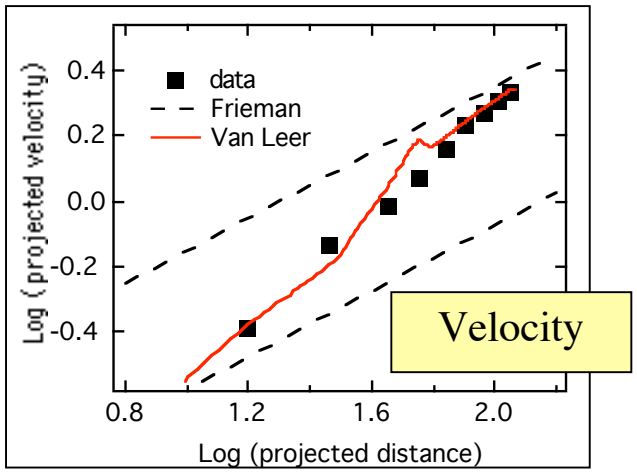

Velocity

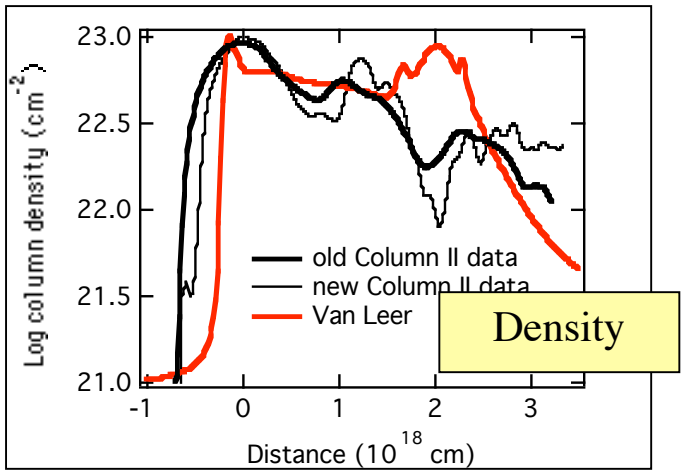

Density

At first sight a pure cometary model seems more difficult to reconcile with observations

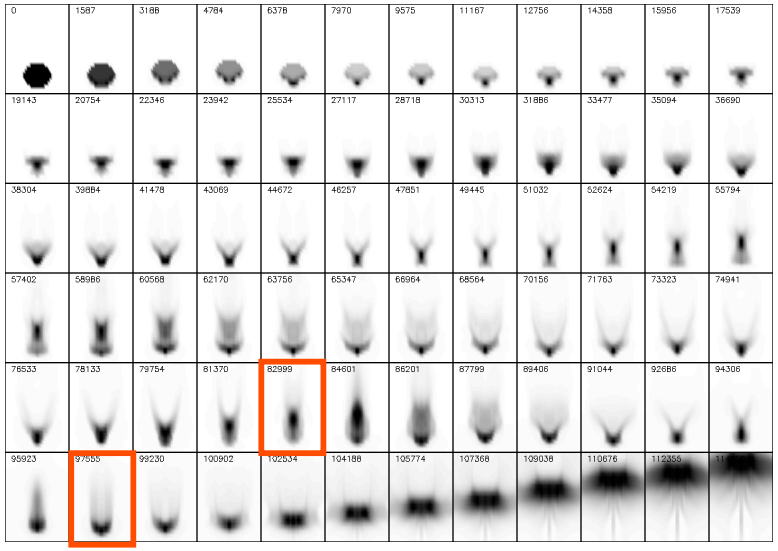

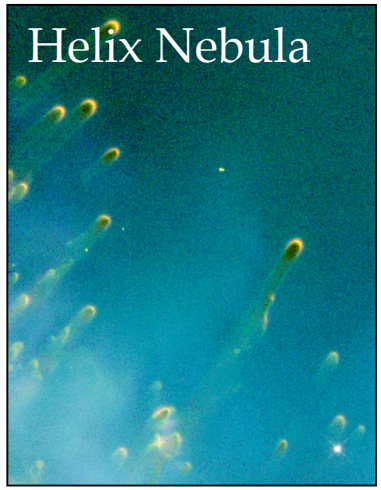

O'Dell, C. R. & Handron, K., AJ 111, 130 (1996)

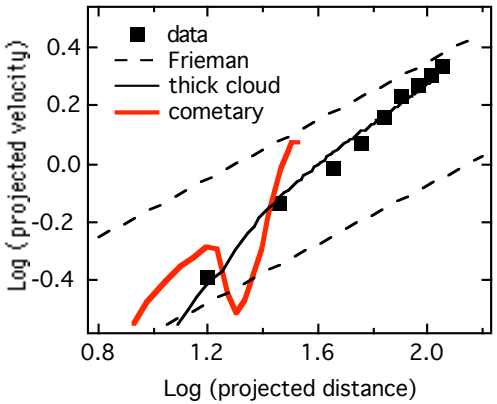

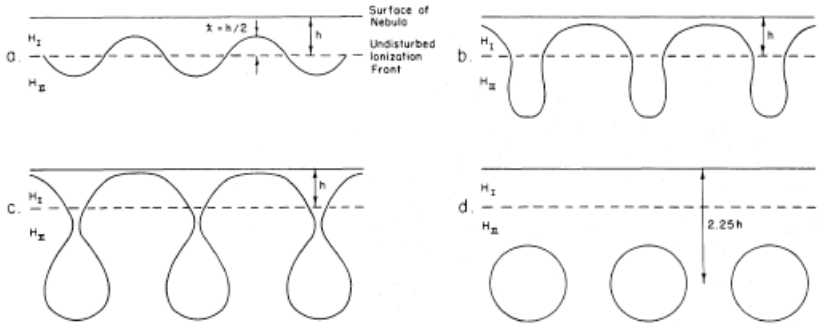

Capriotti, ApJ 179, 495 (1973)

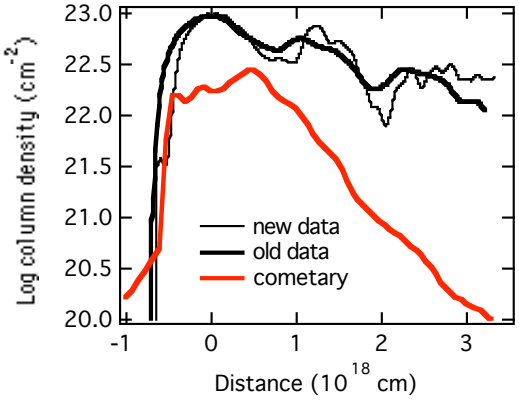

Intermediate ‘dense nuclei’ models are a compelling possibility

Mark McCaughrean and Morten Andersen of the Astrophysical Institute Potsdam (AIP), and the European Southern Observatory (ESO).

Sugitani *et al.*, *ApJ* 565 L28 (2002)

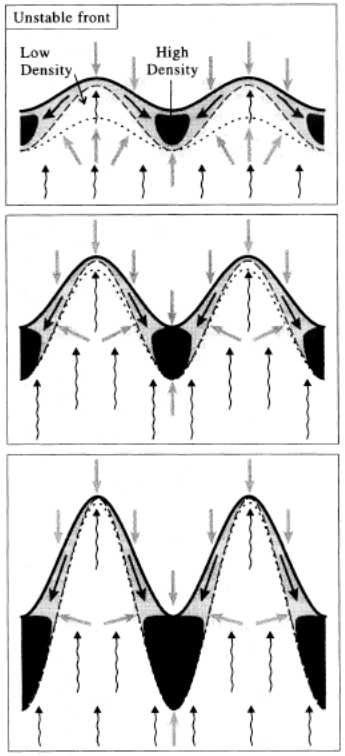

García-Segura and Franco *ApJ* 469 171 (1996)

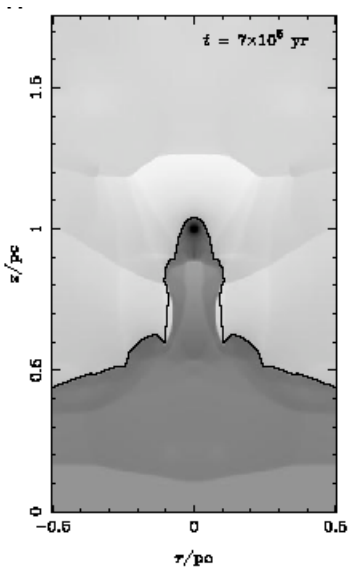

Williams, Ward-Thompson & Whitworth, Mon. Not R. Astron. Soc. 327, 788 (2001)

The evolution of a perturbation in the linear regime varies dramatically, depending on whether or not recombination is included

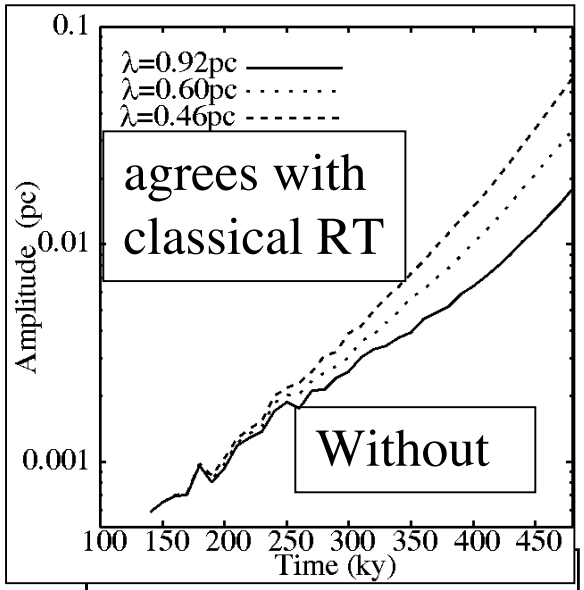

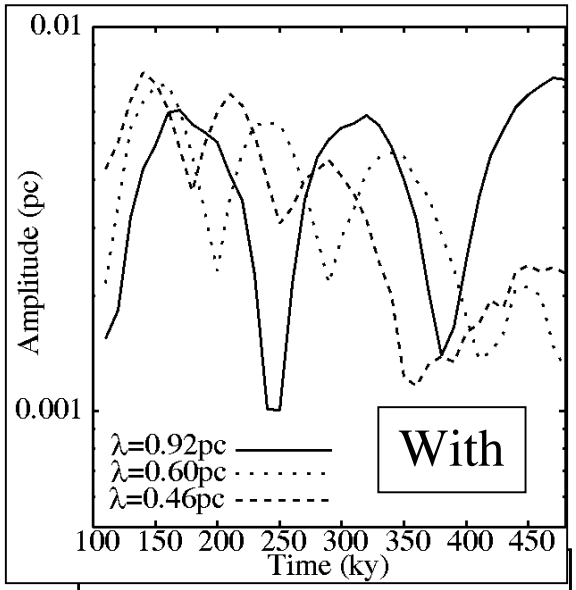

Mizuta *et al.*,ApJ **621**, 803–807, (2005)

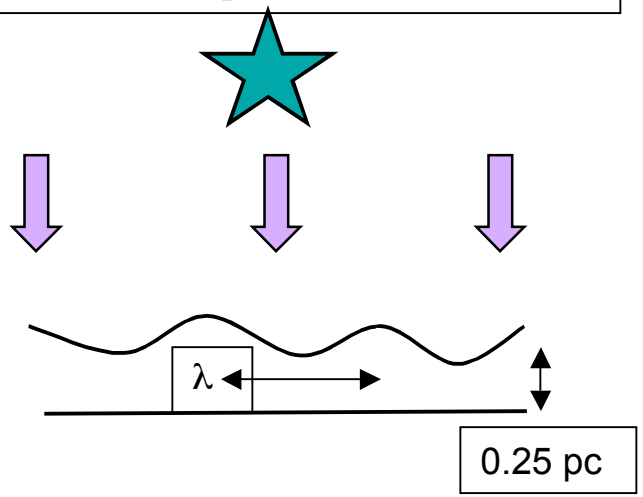

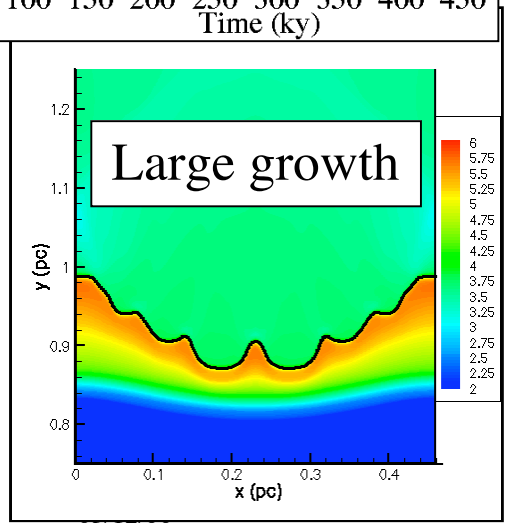

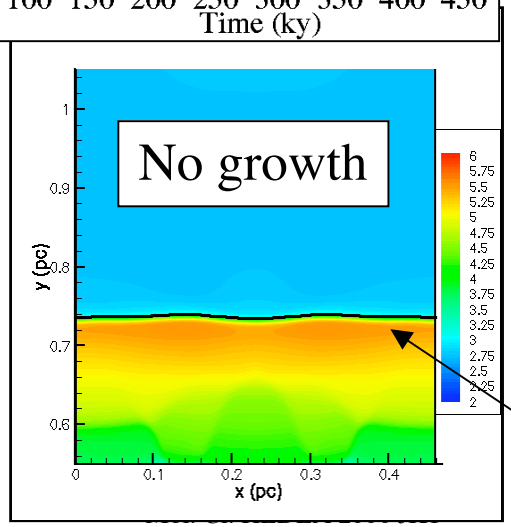

- Perturbation grows in case w/o recombination.
- does not grow w/ recombination.

Log scale number density contour ;in later phase

The effect of including recombination in the linear regime leads to a strong damping of perturbation growth

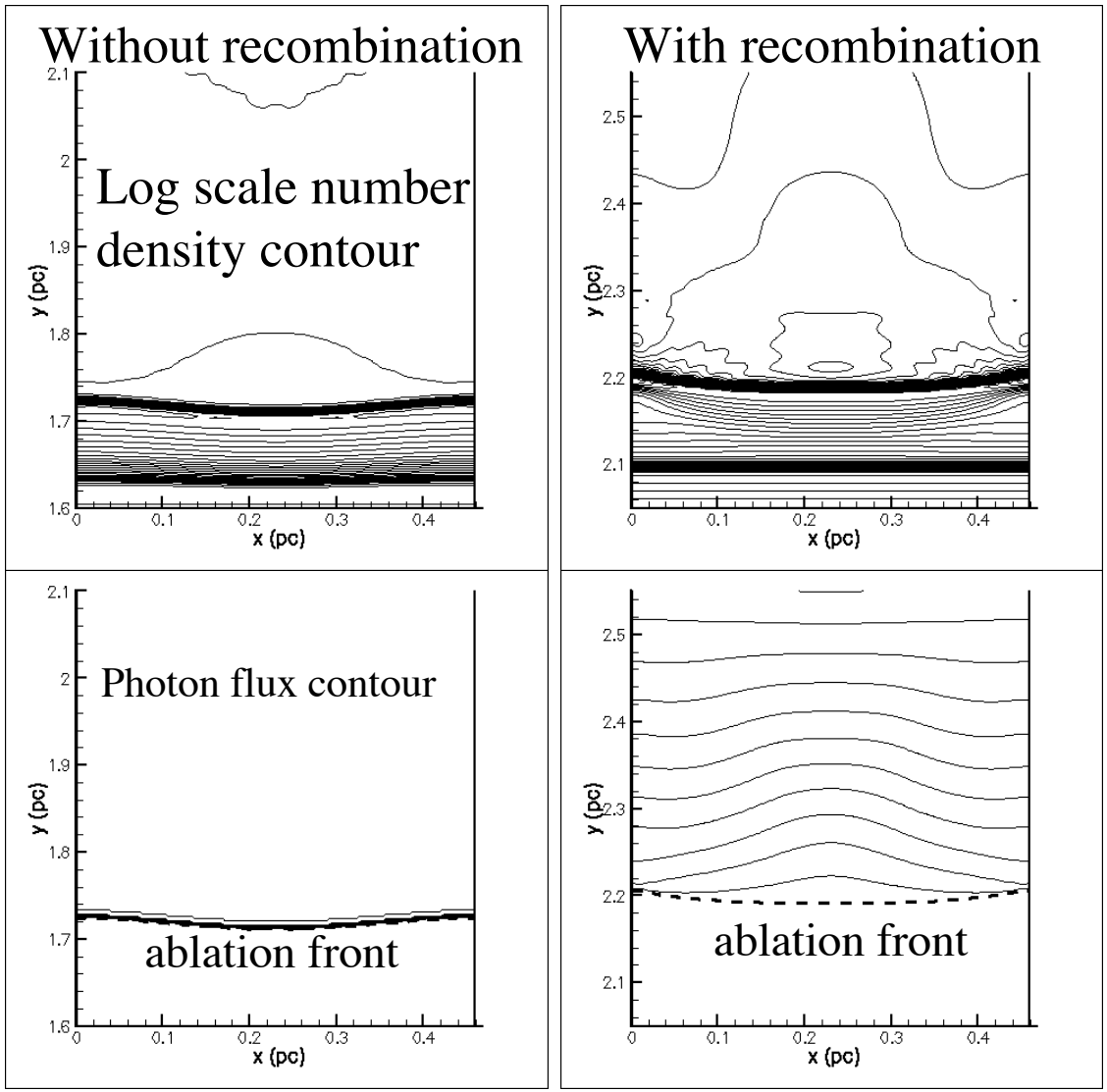

Stabilization mechanism
Concavity
↓
Greater extinction
↓
Reduced ablation pressure

Vandervoort, ApJ **135,** 212 (1962)
Axford, ApJ **140,** 112 (1964)

Absorption profile is quite different, because the recombination rate has dependence on n^2.

With small initial perturbation (linear regime) "ionization damping" dominates: no RT growth

Mizuta Eagle Nebula Pillar II model at 460 ky vs. Pound column density and velocity data

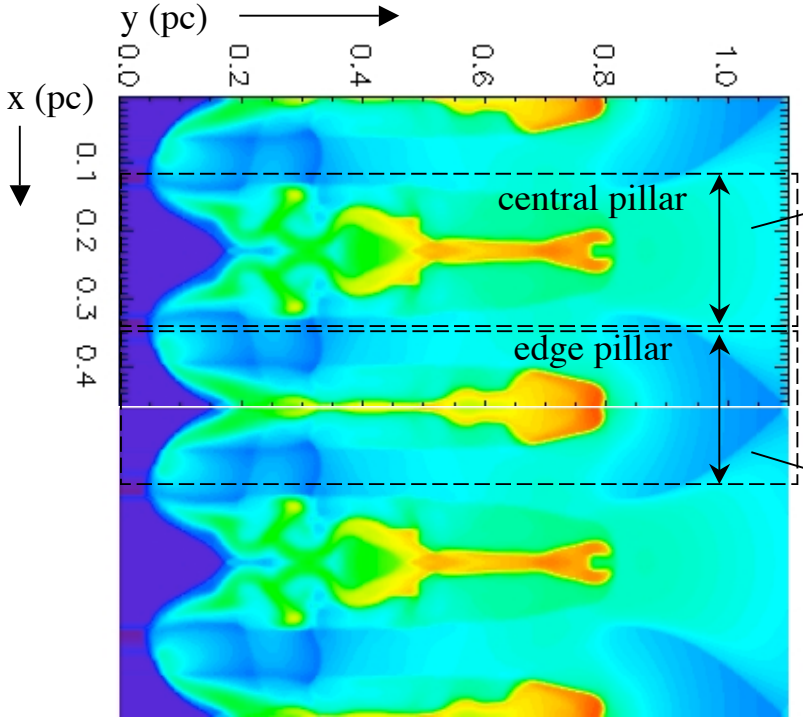

log_10 density contours in model

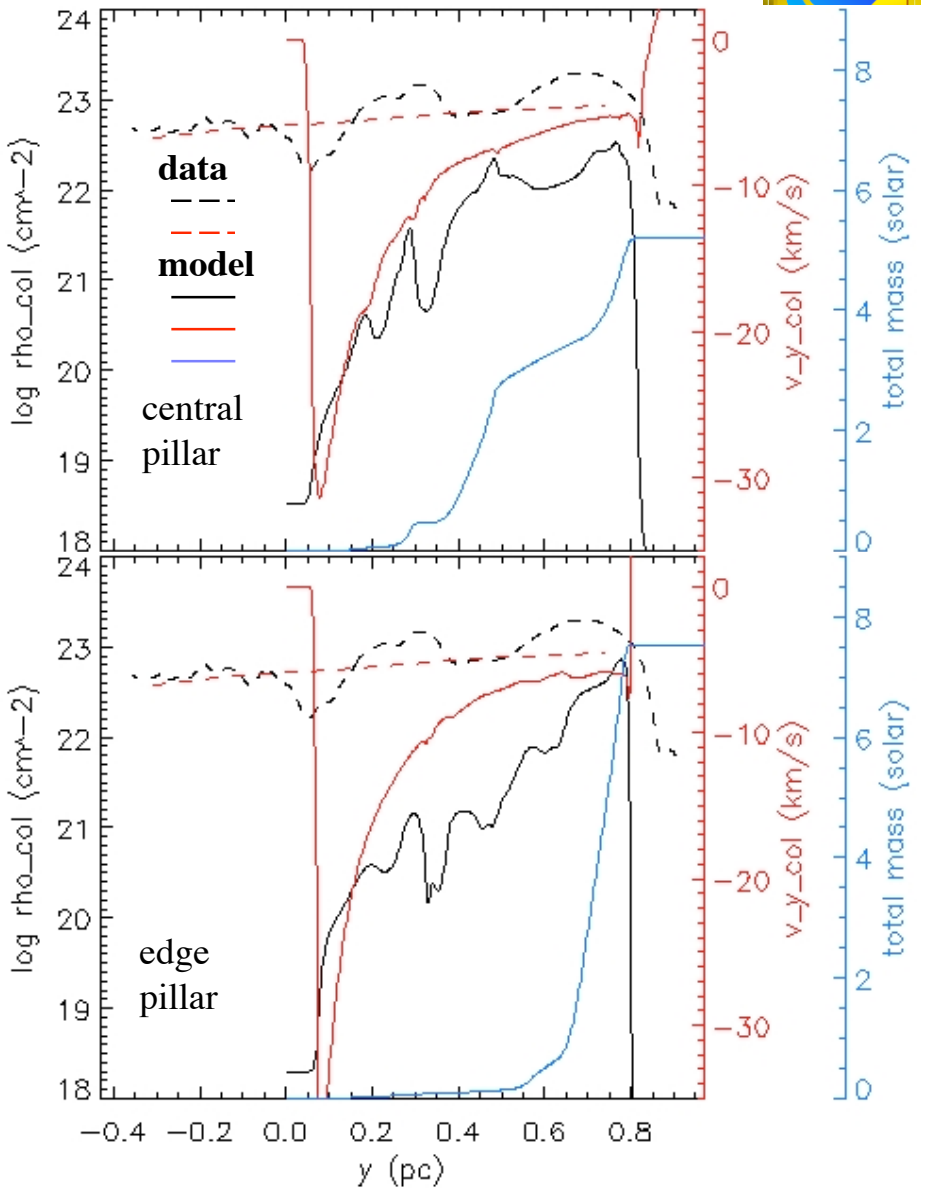

optically thin column density and velocity:

$n\_H2(x,y) = [1-f(x,y)] \times rho(x,y) / m\_H2$

$rho\_col(y) = \int n\_H2(x,y)\, dx$

$v\_y\_col(y) = \int n\_H2(x,y) \times v\_y(x,y)\, dx / rho\_col$

$dmass = 2\pi\, (x-x_0)\, dx\, dy\, n\_H2(x,y) \times m\_H2$

Mizuta Eagle Nebula Pillar II model at 400 ky vs. Pound column density and velocity data

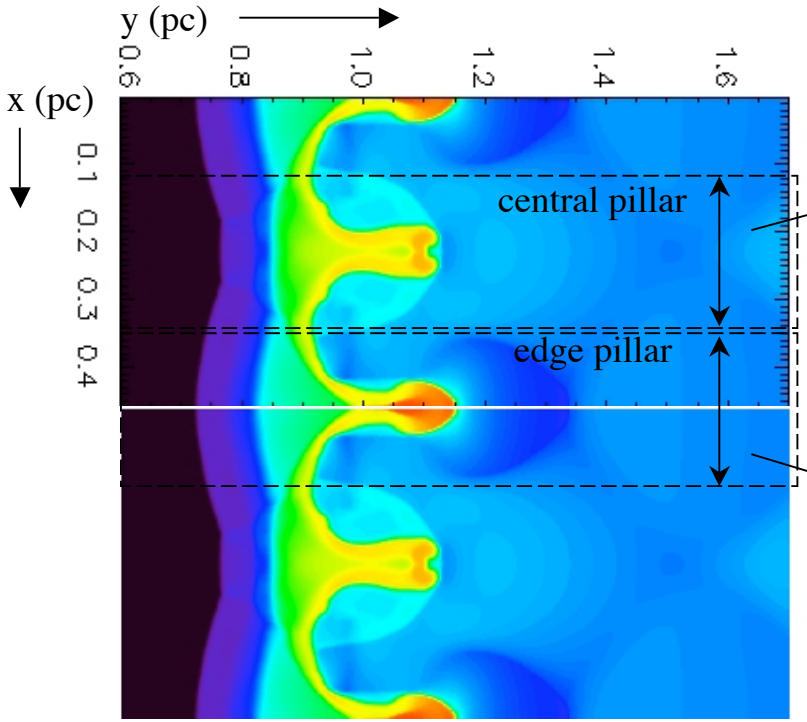

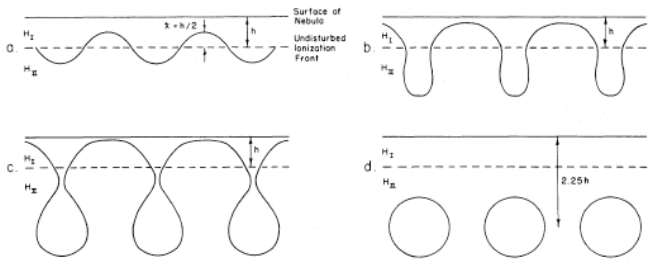

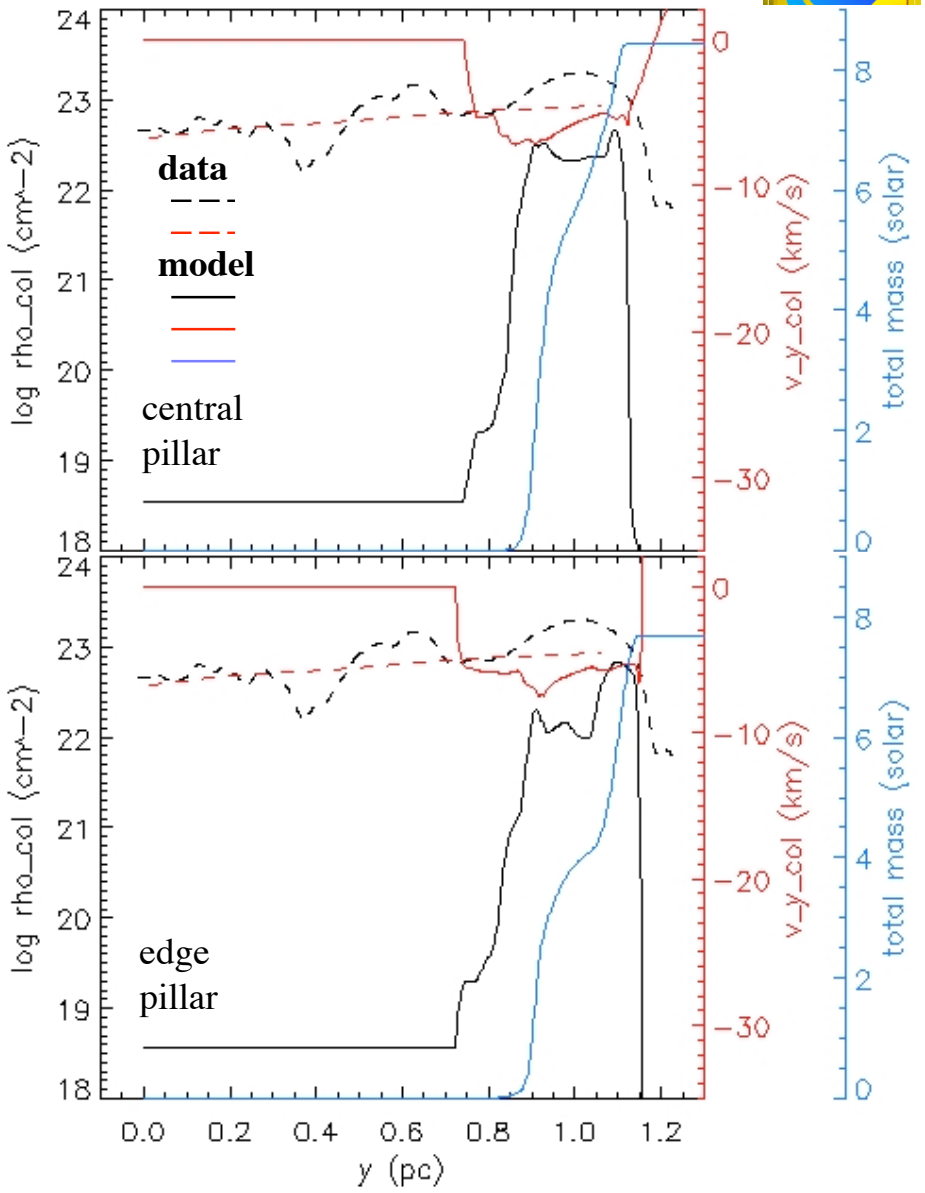

Helix Nebula
Capriotti, ApJ **179**, 495 (1973)

In the absence of recombination, and without acceleration, the Directed Radiation instability can seed significant non-linear structure that grows by shadowing.

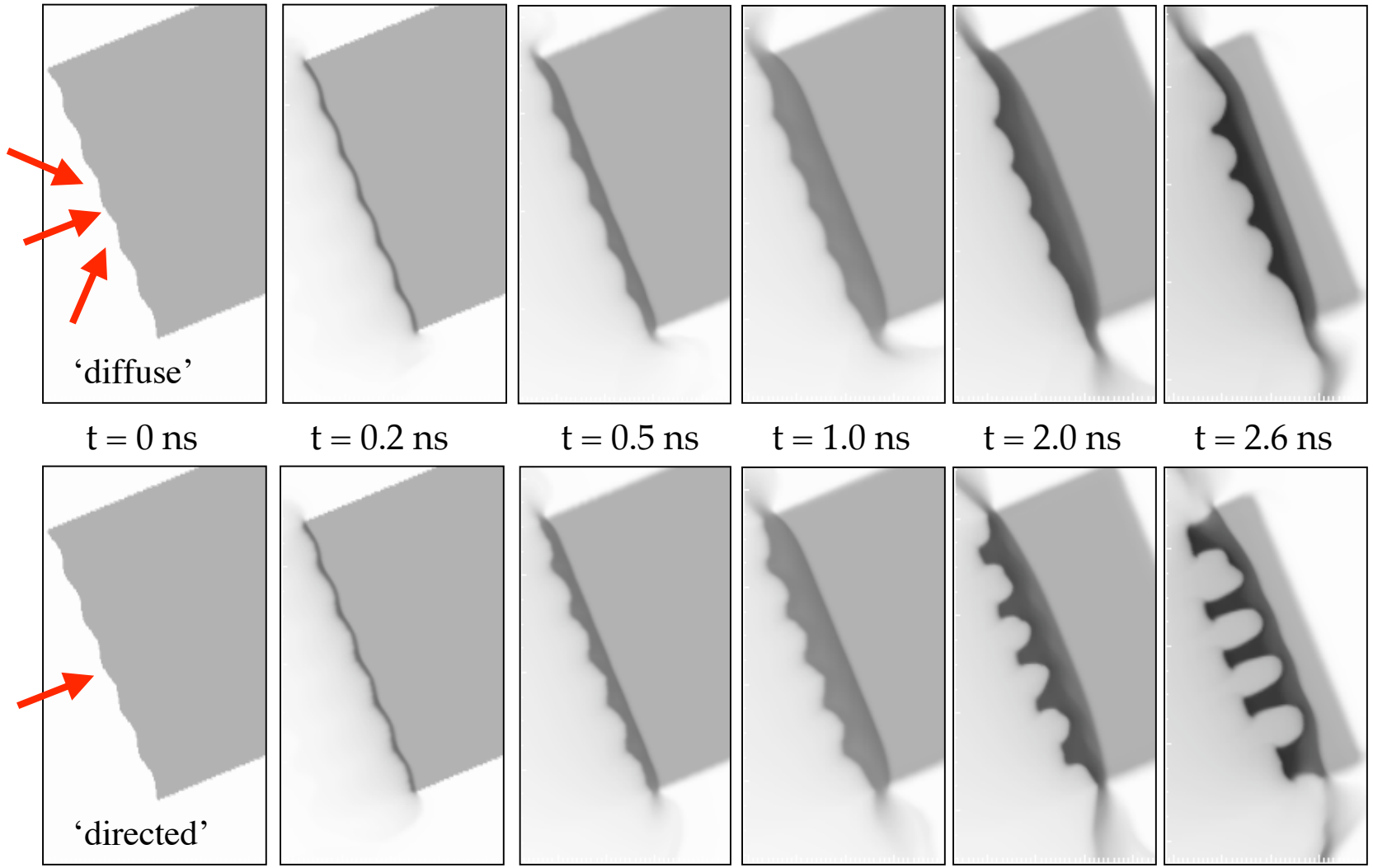

$\lambda = 10\ \mu m$, $\eta_0 = 0.5\ \mu m$ and the target turned by $\pi/8$ on the grid and tabular EOS

With a **flat** interface turned on the grid, stairstepping leads to growth of $l \approx 8$ mm with directed radiation, which leads quickly to a disrupted shell in the acceleration phase

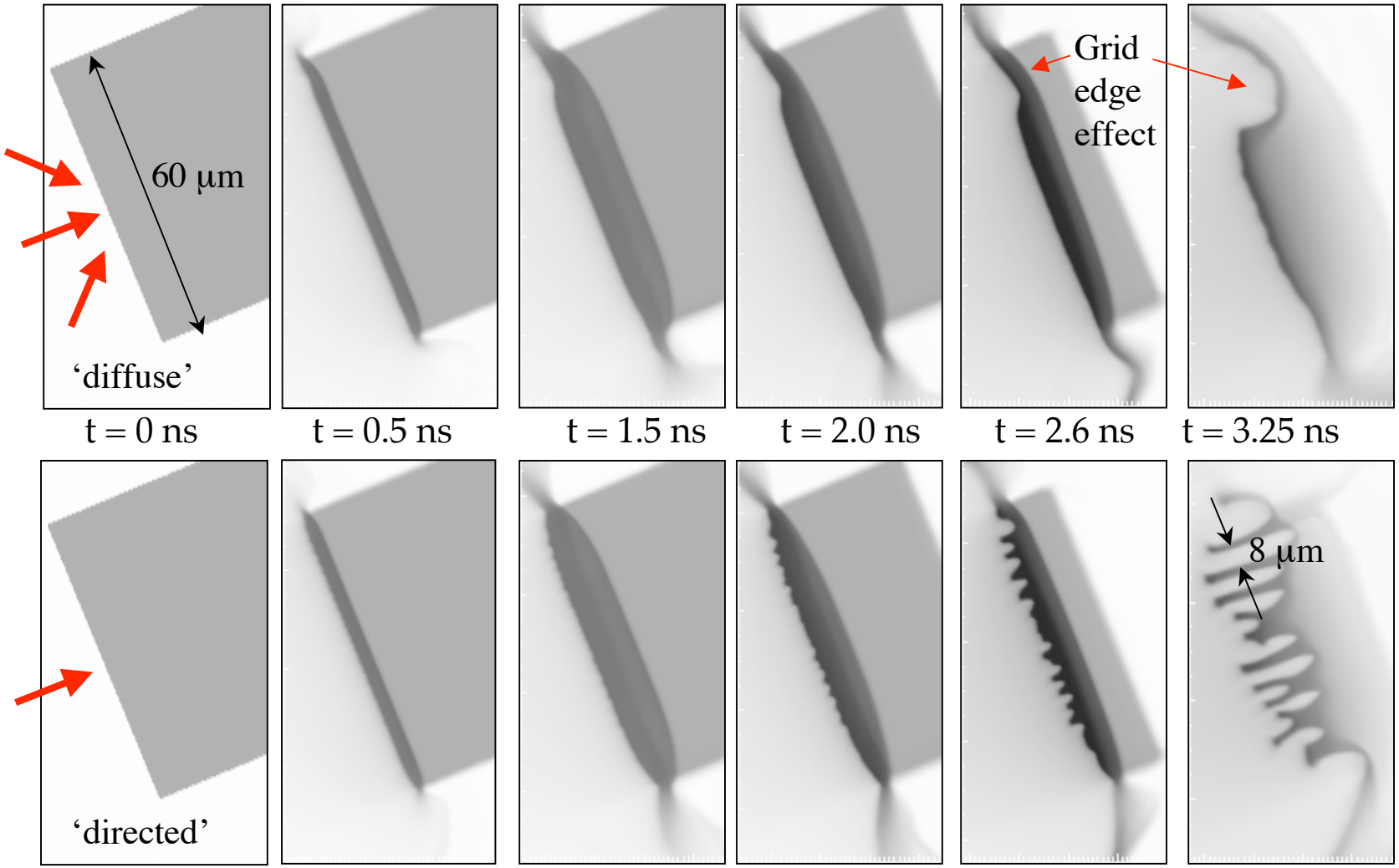

Next we consider RT and cometary models using divergent rays and large cylindrical volume to allow diverging outflow

Grid and rays (schematic)

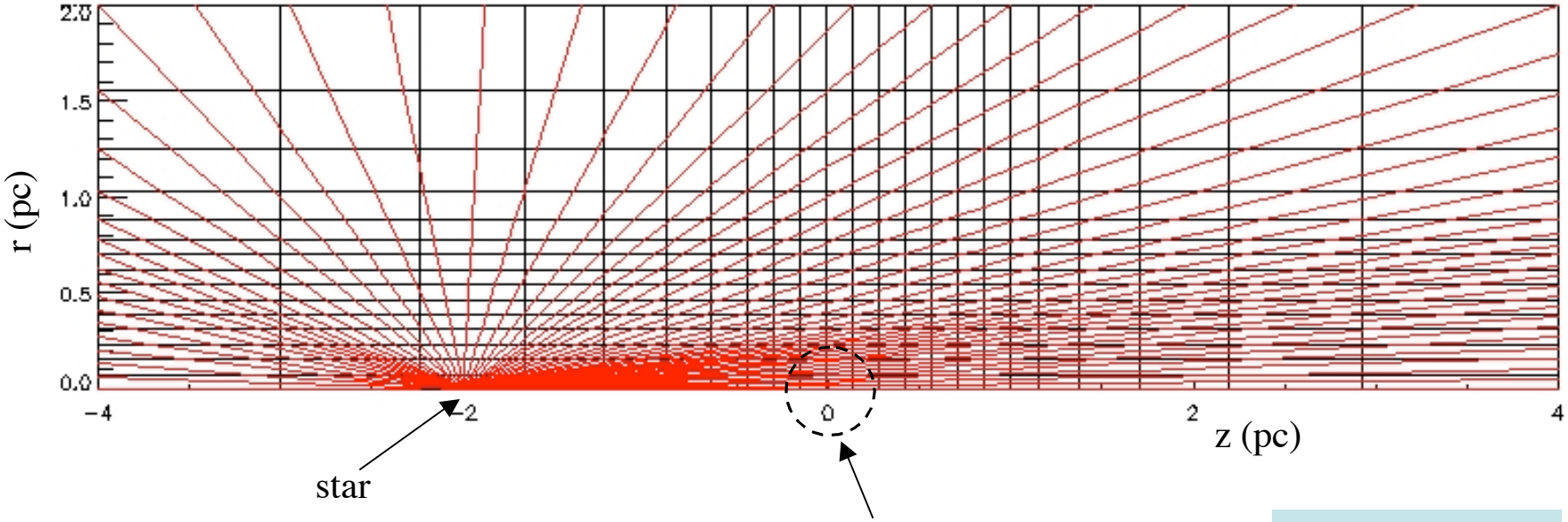

- $dJ/dr = -a\, n\, (1-f)\, J \quad -3\, J\, /r$

divergence

Refs.
Richfield, Yorke, etc.
Stone, Norman (Zeus)

Lefloch & Lazareff
1994 A&A, 289, 559
1995 A&A, 301, 522

- Weighted averages are used for *df* in zones crossed by multiple rays

• I use Akira's spatial resolution in the cloud, and his EOS. I use his initial thermal and magnetic pressure, with modification in the cometary core (below). I use his molecular cooling rate.

• The star luminosity is 1.2e50 photons/s.

• For the cometary simulations the initial cloud is spherical with a power law density profile. I've tried various profiles, attempting to match the visible morphology and Marc's data. I limit the initial p_M(r,z) in the core so that the cloud and surrounding material are in pressure equilibrium. The initial star is 2 pc from the core.

• For the RT simulations, I use Akira's thin cloud parameters, but with finite lateral extent, as suggested by ground based images. The initial star is 1.5 pc from the core, since the cloud will move. I show a case with a 25% initial density perturbation. I've also tried dropping the central flux for 10 kyr at the start of the acceleration phase, as Akira did, and I've tried no perturbation; the results are all similar.

RT model

Star at z = -1.5 pc

The RT simulations show no growth, although a cometary shape might slowly be reached. Ray divergence means the center is pushed harder, but the edges see increased flux due to outflow divergence.

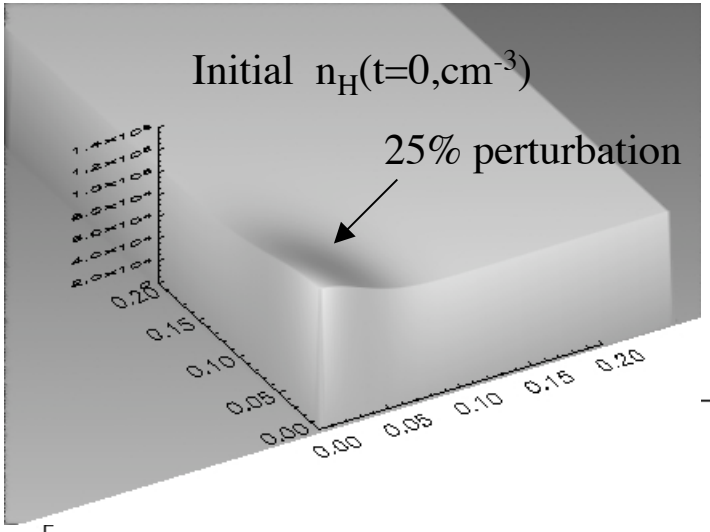

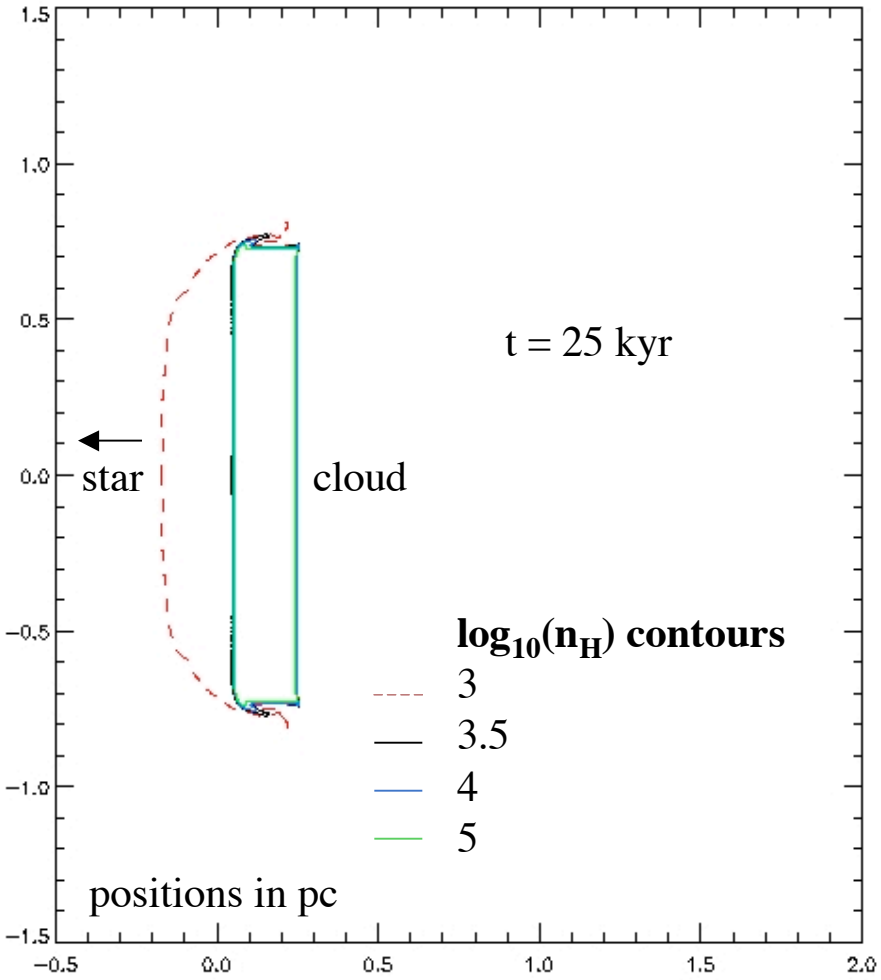

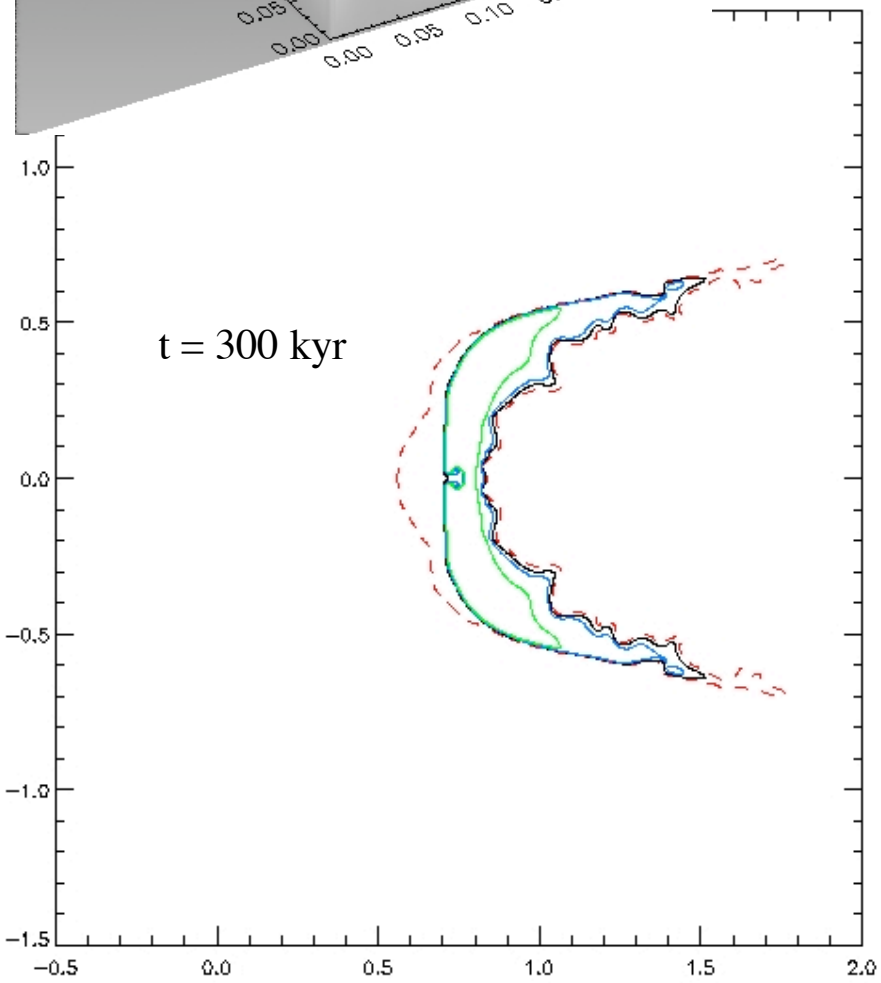

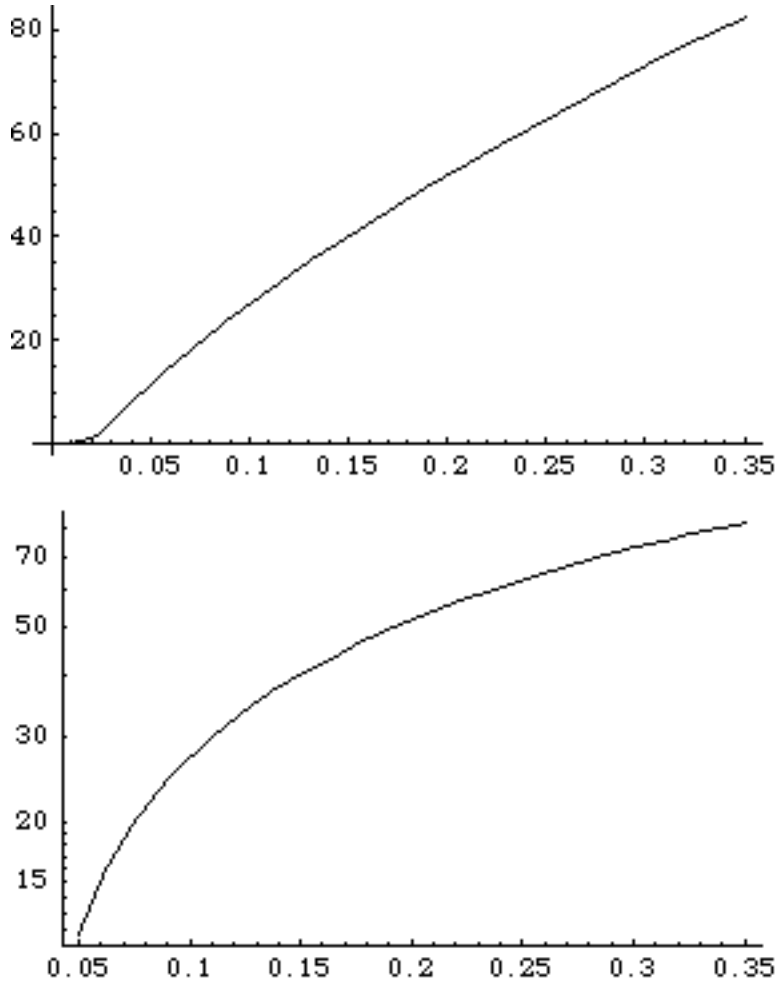

$M(r)/M_{sol}$

R(pc)

Initial log_10 $n_H(z, r=0, cm^{-3})$

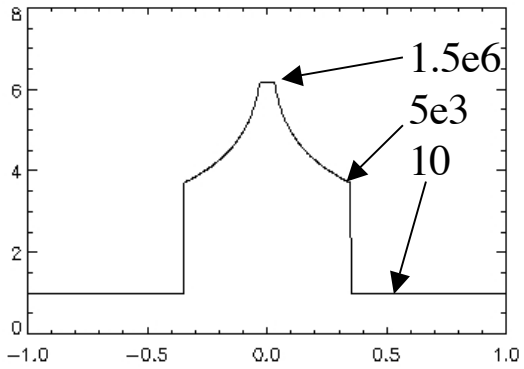

z (pc)

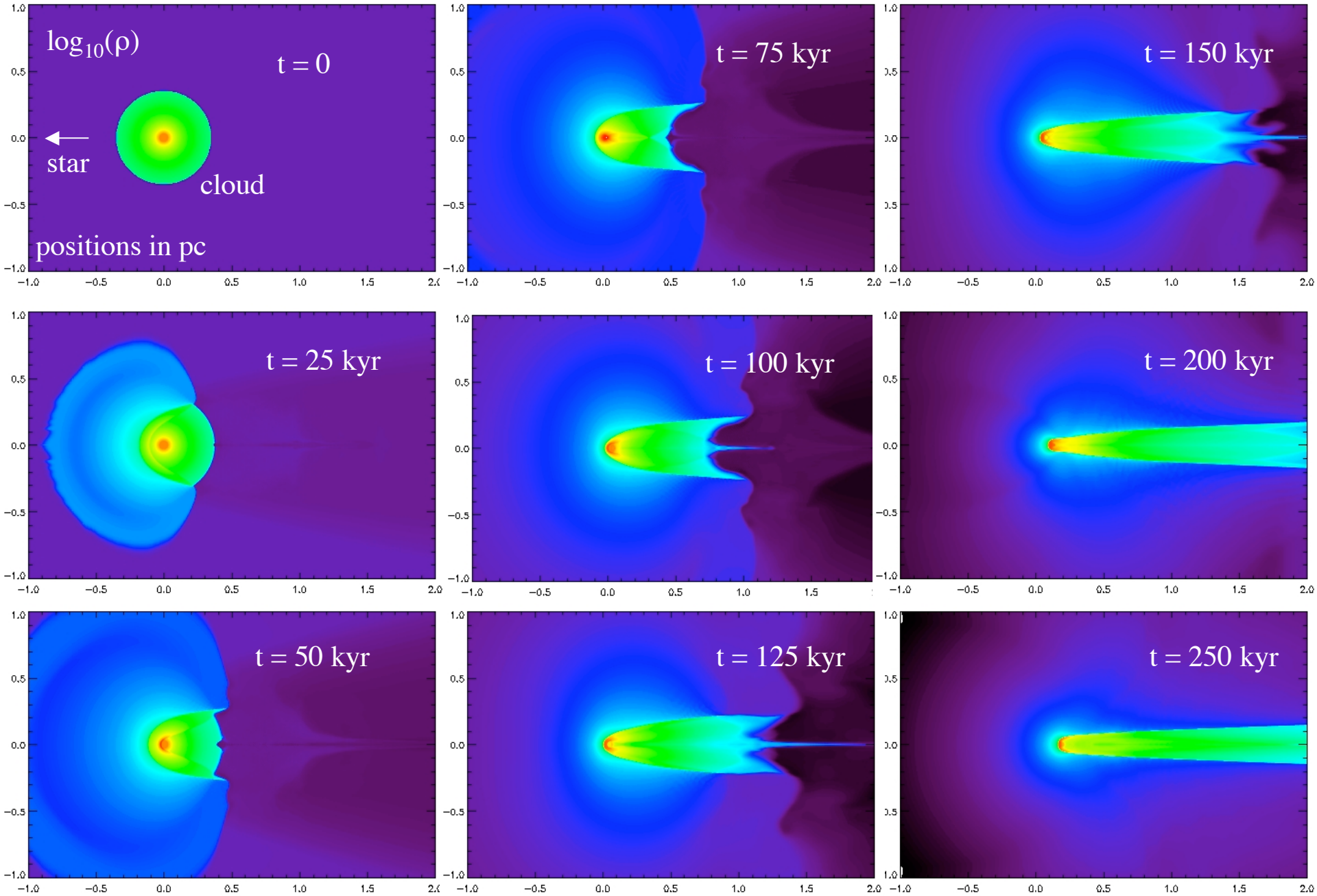
log10(ρ)
t = 0
star
cloud
positions in pc
t = 75 kyr
t = 150 kyr
t = 25 kyr
t = 100 kyr
t = 200 kyr
t = 50 kyr
t = 125 kyr
t = 250 kyr

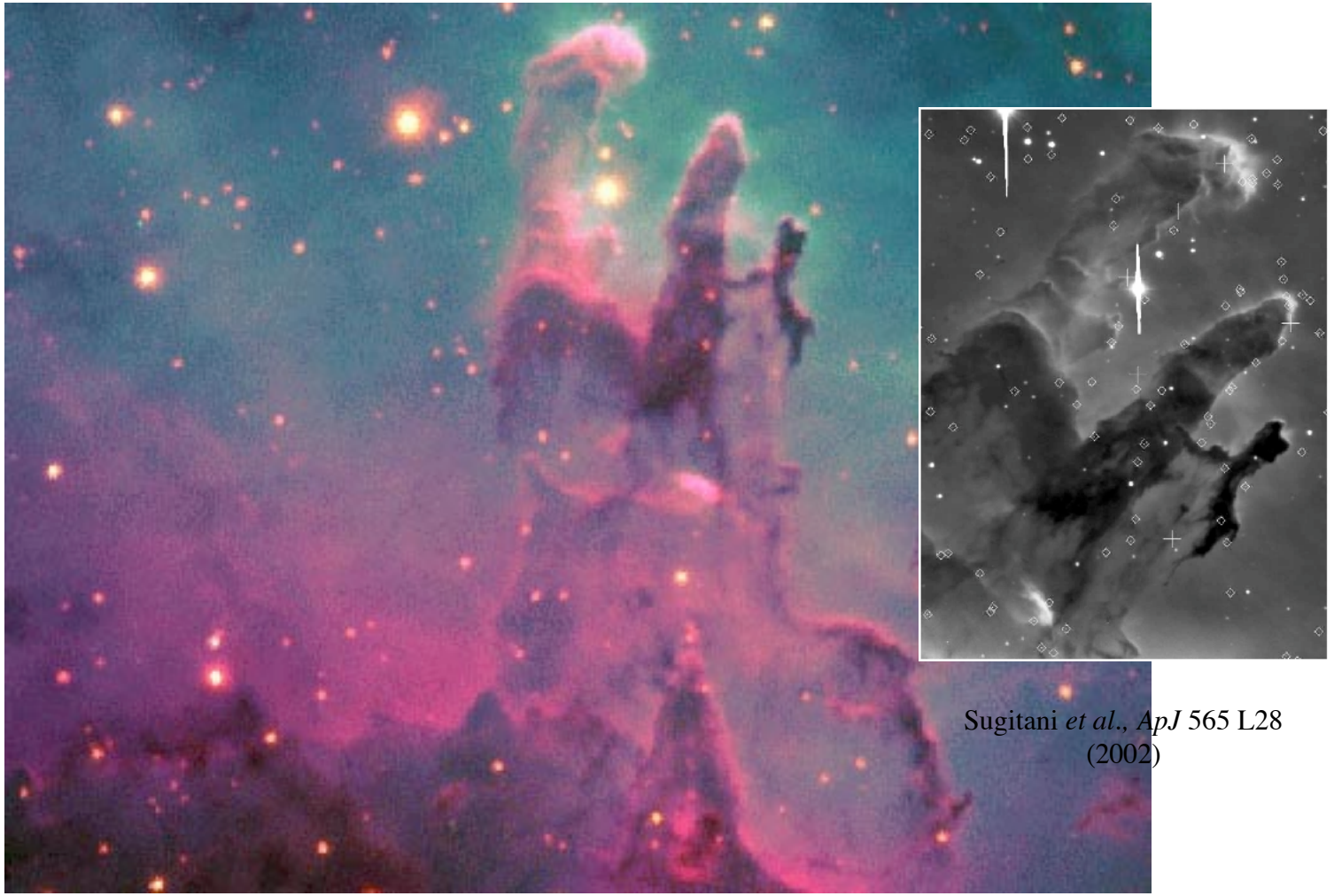

Sugitani *et al.*, *ApJ* 565 L28 (2002)

Star at z = -2 pc

t = 250 kyr, projection angle 20°

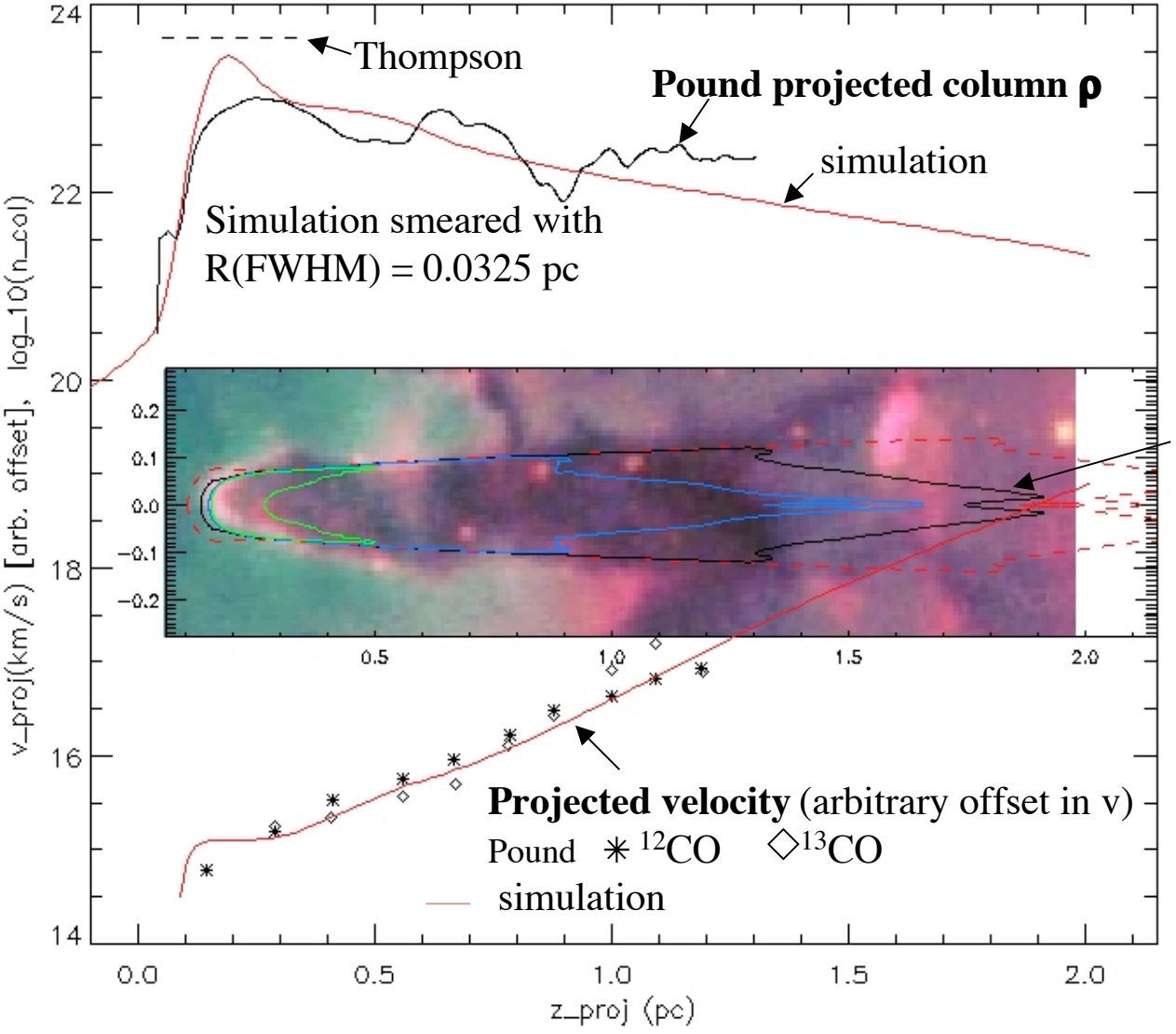

Initial n_H(z, r=0, cm^{-3})

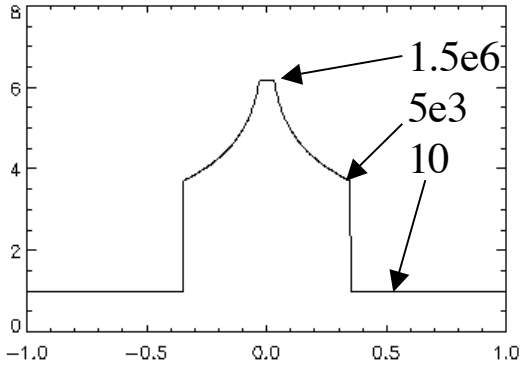

Simulated $\log_{10}(n_H)$ contours

3
3.5
4
5

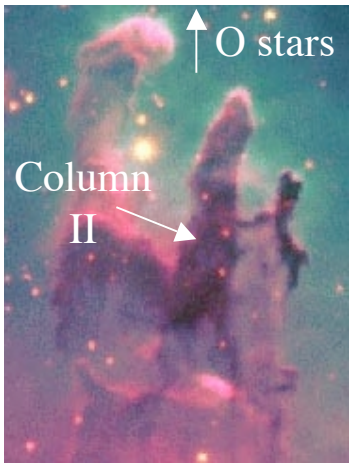

ground-based image

r(pc)

$\log_{10}(p/k)$

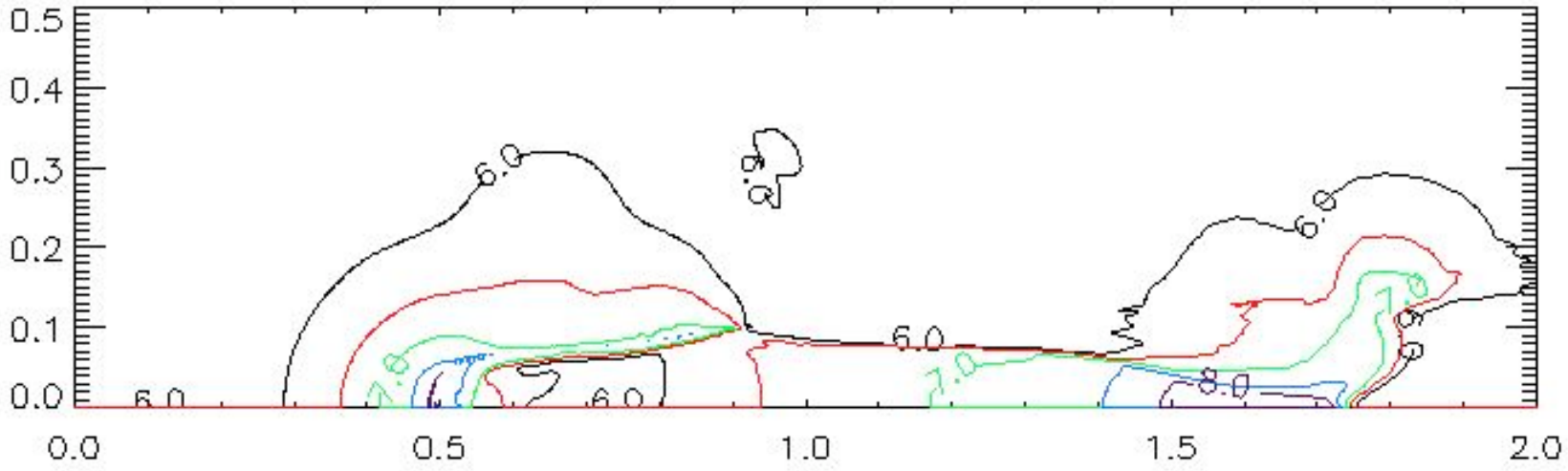

z(pc)

- The cometary model does well in velocity gradient and morphology.

- The tip column density is higher than Marc's but actually lower than suggested by Thompson et. al for Column I (2002 ApJ, 570, 749).

- The density in the extreme tail is lower than Marc's, but the ground based image suggests there is other material in the line of sight.

- It appears difficult to both match Marc's tip density and throw enough material into the extreme tail. To approach Marc's density in the extreme tail, it seems the head must be massive to stay back while the tail forms. Clumpiness of the actual initial cloud, unknown line-of-sight structure, and the large wiggles in Marc's data should be kept in mind.

- Other points:

(1) The cometary model predicts a long, low-density (< 1e3 /cc) extension to the tail, rather than a sharp cutoff. The ground-based image may show wispy (limb-darkened?) hints of this. Or, the tail may have collided with denser material. Could observations help?

(2) The tail radius fluctuates as material converges on axis behind the head and rebounds; magnetic pressure and molecular cooling appear to damp this fluctuation.

(3) Like cooling, the magnetic pressure appears to be numerically unstable.

(4) The diverging outflow reaches the snowplow phase and stalls inside the simulation boundaries.

The dense intial nucleus holds the comet back

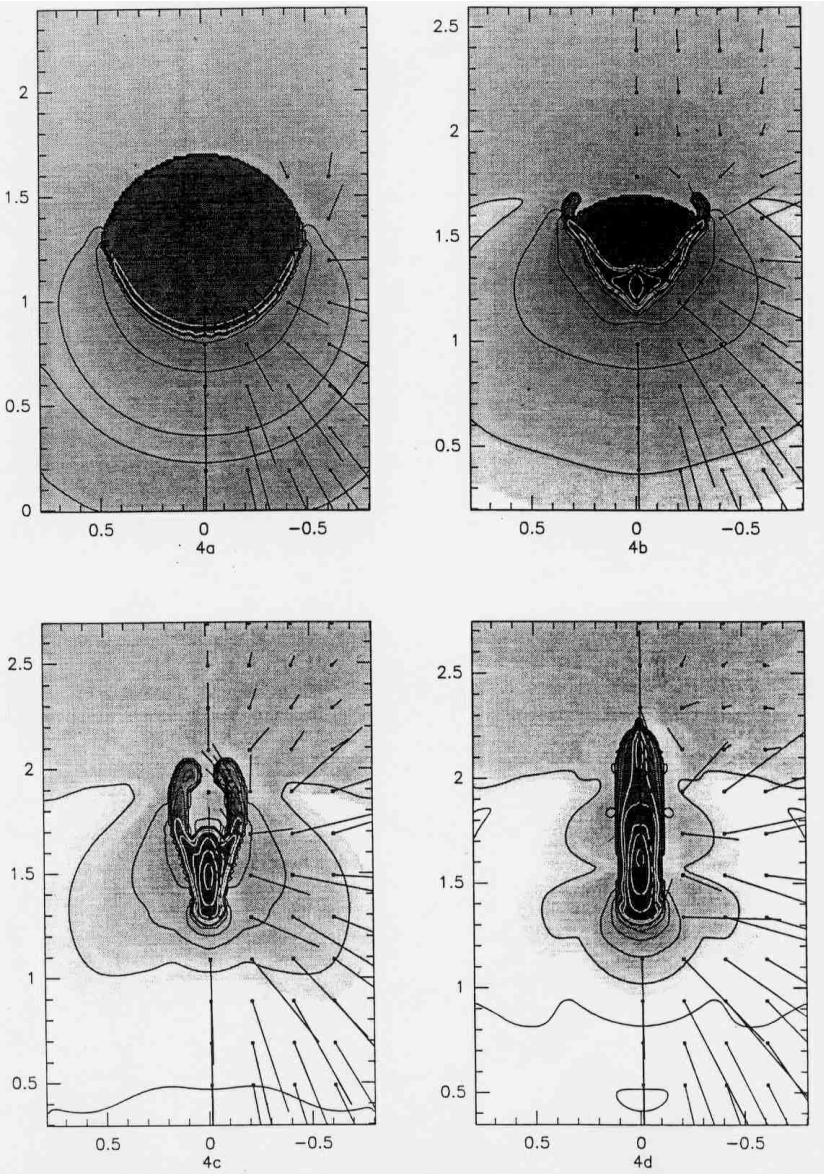

Lefloch & Lazareff, A&A **289**, 559 (1994);

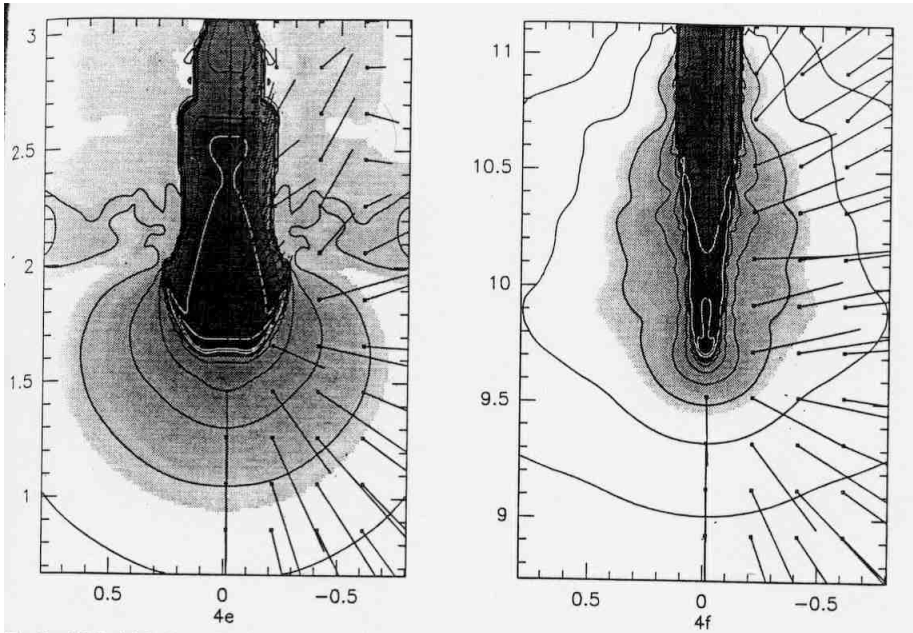

Fig. 4e–f. Model 2: Reexpansion stage (t = 0.37 My **e**) and cometary phase (t = 1.30 My **f**)

Cometary model of Eagle Nebula Column II

Star at z = -2 pc

t = 500 kyr, projection angle 25°

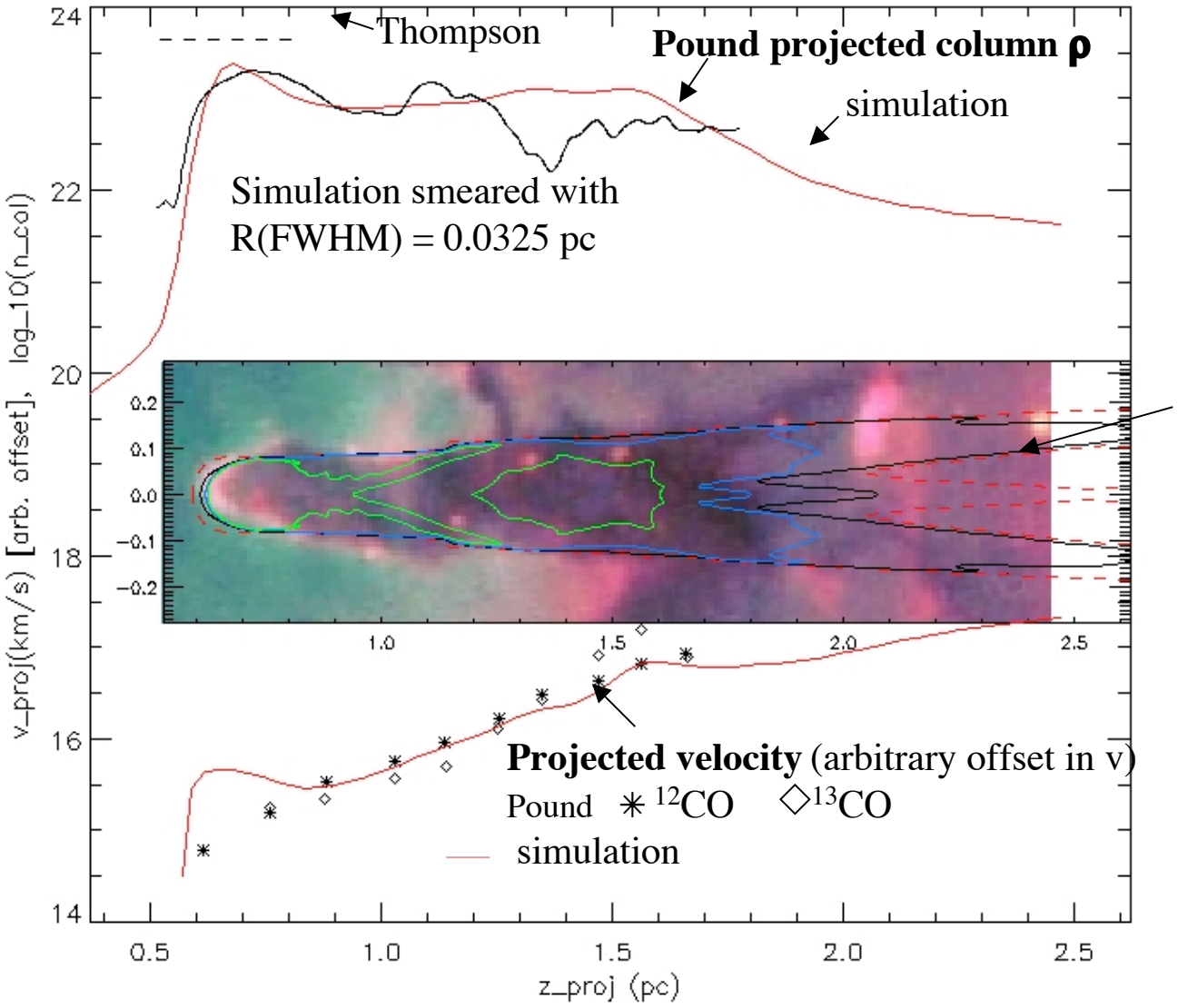

Initial n_H(z, r=0, cm^{-3})

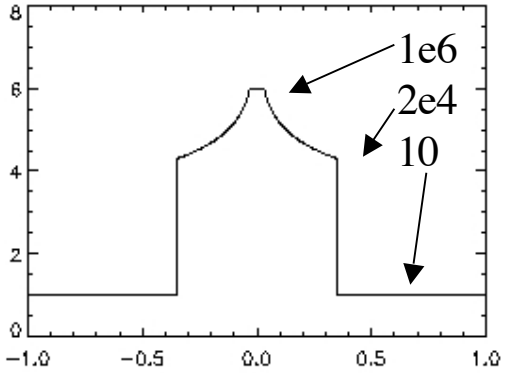

Simulated $\log_{10}(n_H)$ contours

- 3
- 3.5
- 4
- 5

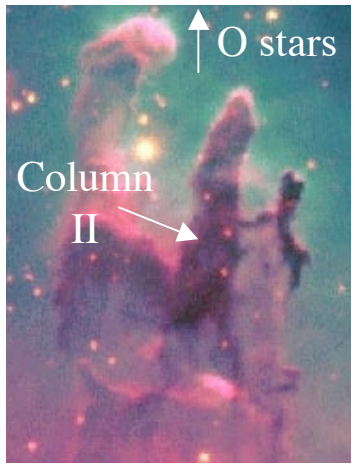

ground-based image

Cometary model of Eagle Nebula Column II

Star at z = -1.75 pc

t = 425 kyr, projection angle 26°

Initial $n_H(z, r=0, cm^{-3})$

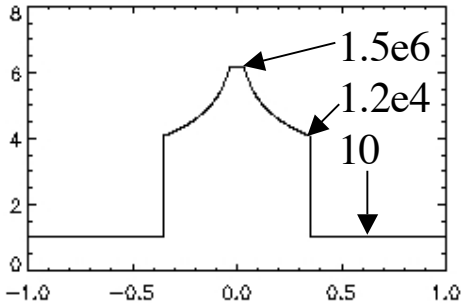

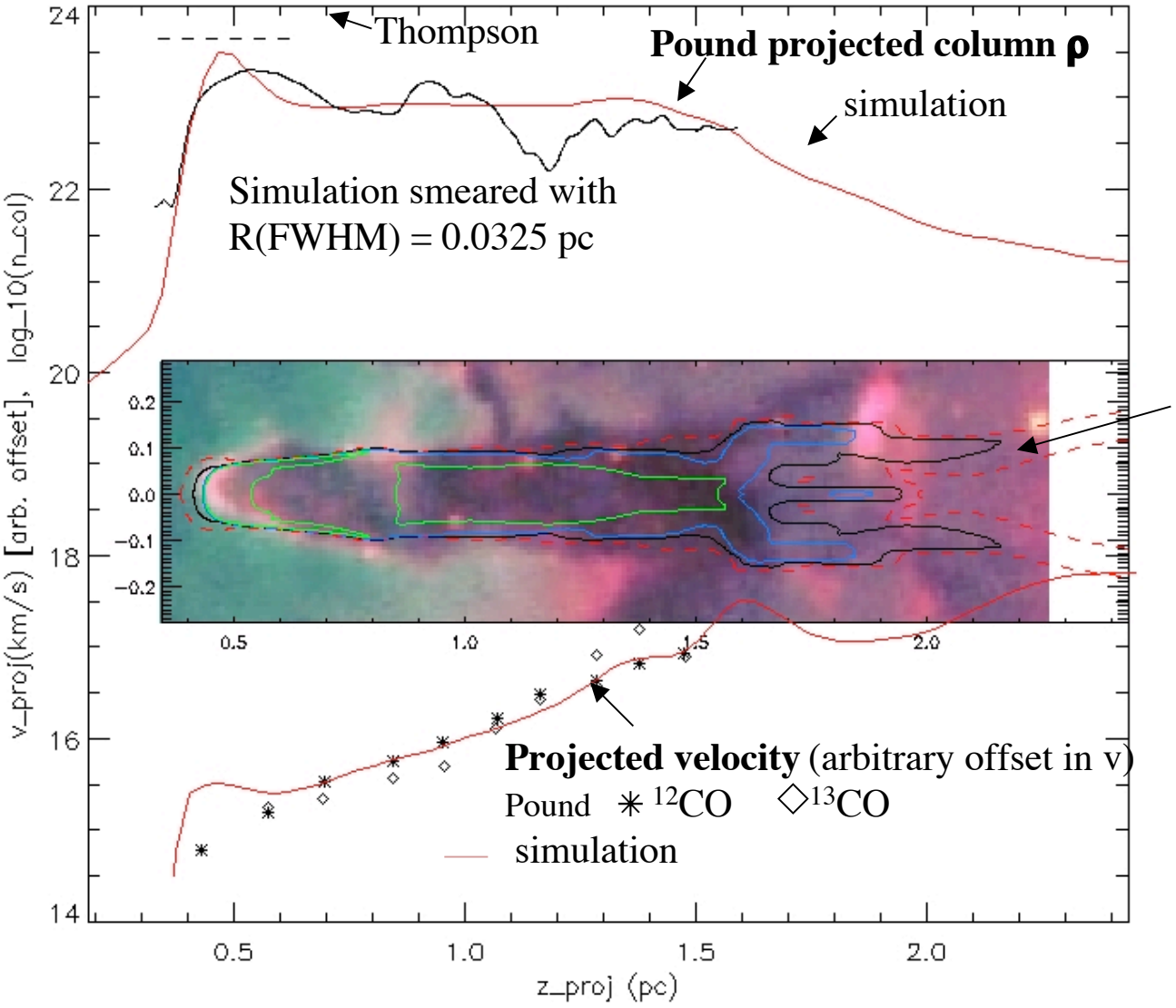

Simulated $\log_{10}(n_H)$ contours

3
3.5
4
5

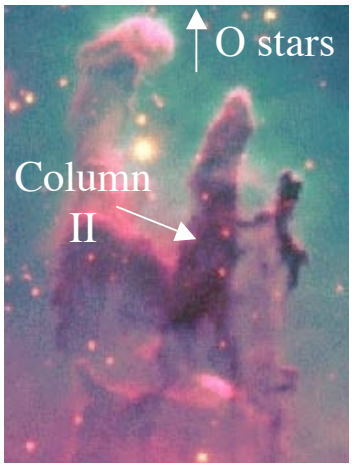

ground-based image

With recombination, cometary models appear to do much better than RT models in explaining Column II of the Eagle Nebula

- There is no RT growth in the linear or nonlinear stages, with a cloud of infinite or finite lateral extent.
- Cometary models with a dense initial core appear to do well on morphology, projected column density, and projected velocity, even with simple treatment of deposition, cooling, and magnetic support pressure, and with the on-the-spot approximation, ignoring diffuse radiation (recombination to the ground state)
- Cometary models are simpler — symmetric, no assumptions about orientation or initial perturbation

Can you produce 'Pillars' by illuminating dense rods embedded in a C foam or CH ablator with direct drive?

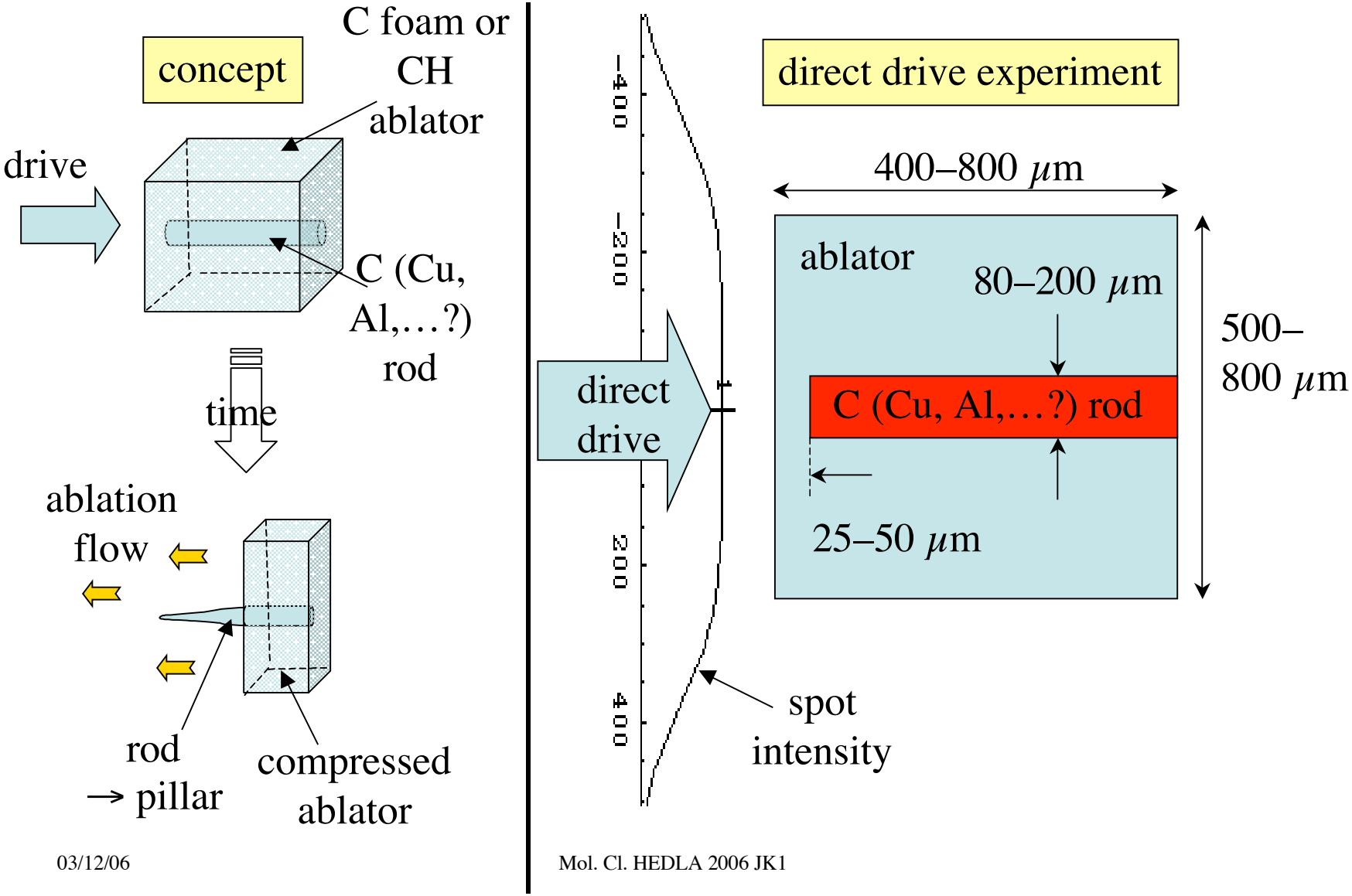

Next we try larger density ratio and structures: a 200 μm diameter C rod in 0.25 g/cm^3 C foam in CALE

Drive:
2400 J, 8 ns flat

Reflect away half of energy at critical surface

Spot: SG8
I~ exp[-(r/411 μm)$^{4.6}$]

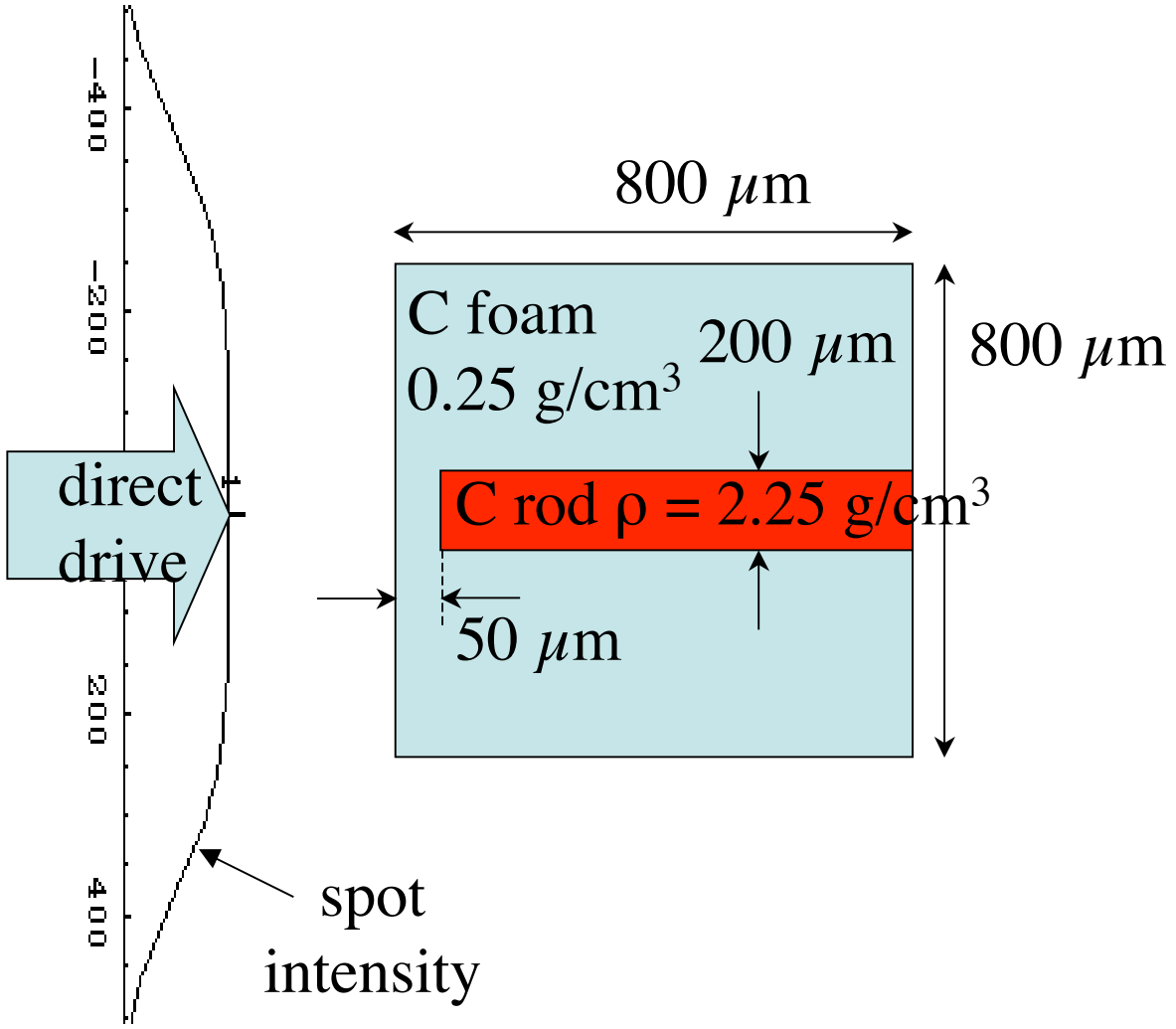

simulated Radiographs 20 μm blurring

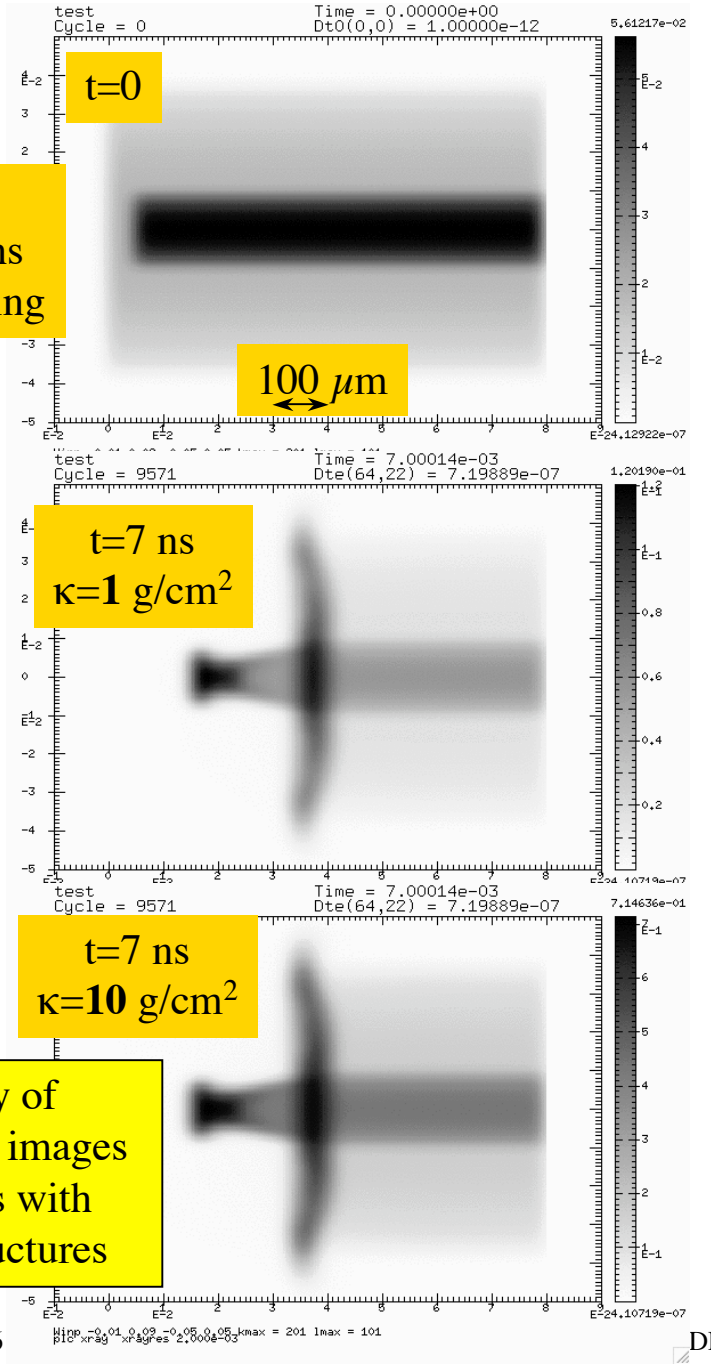

Quality of radiograph images improves with larger structures

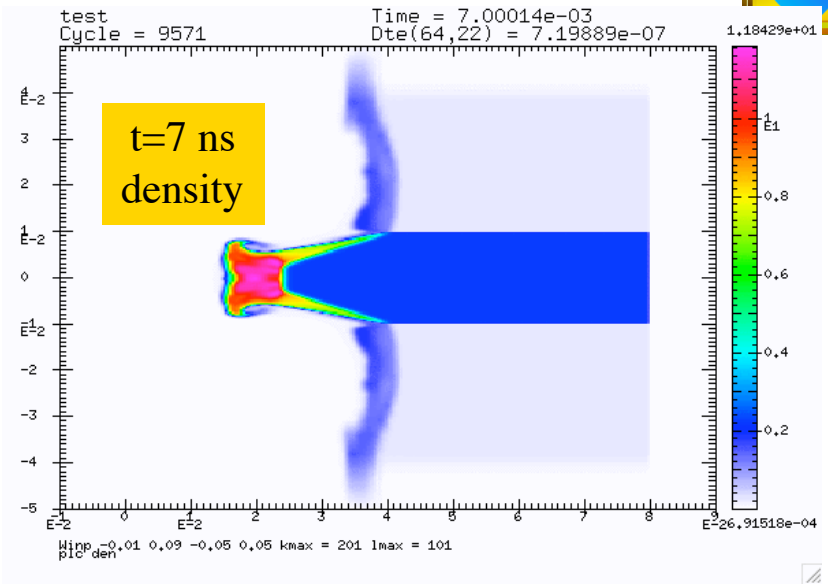

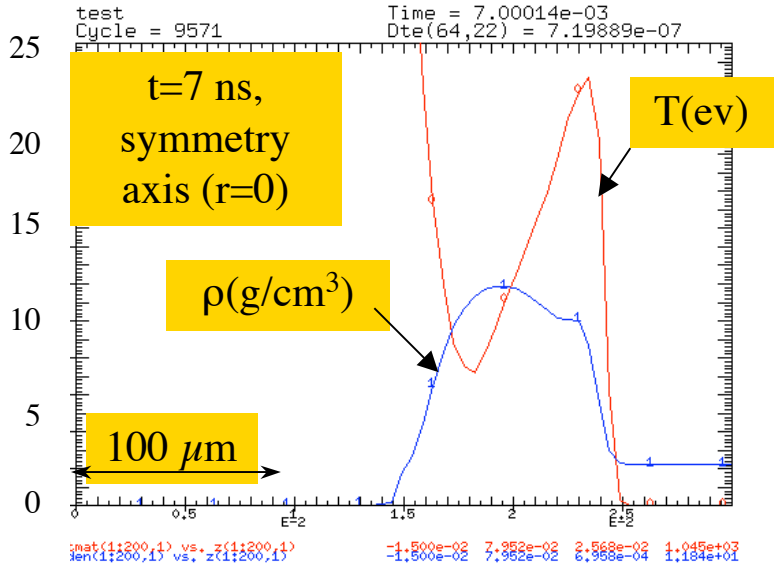

To investigate directional drive, we are considering indirect drive designs

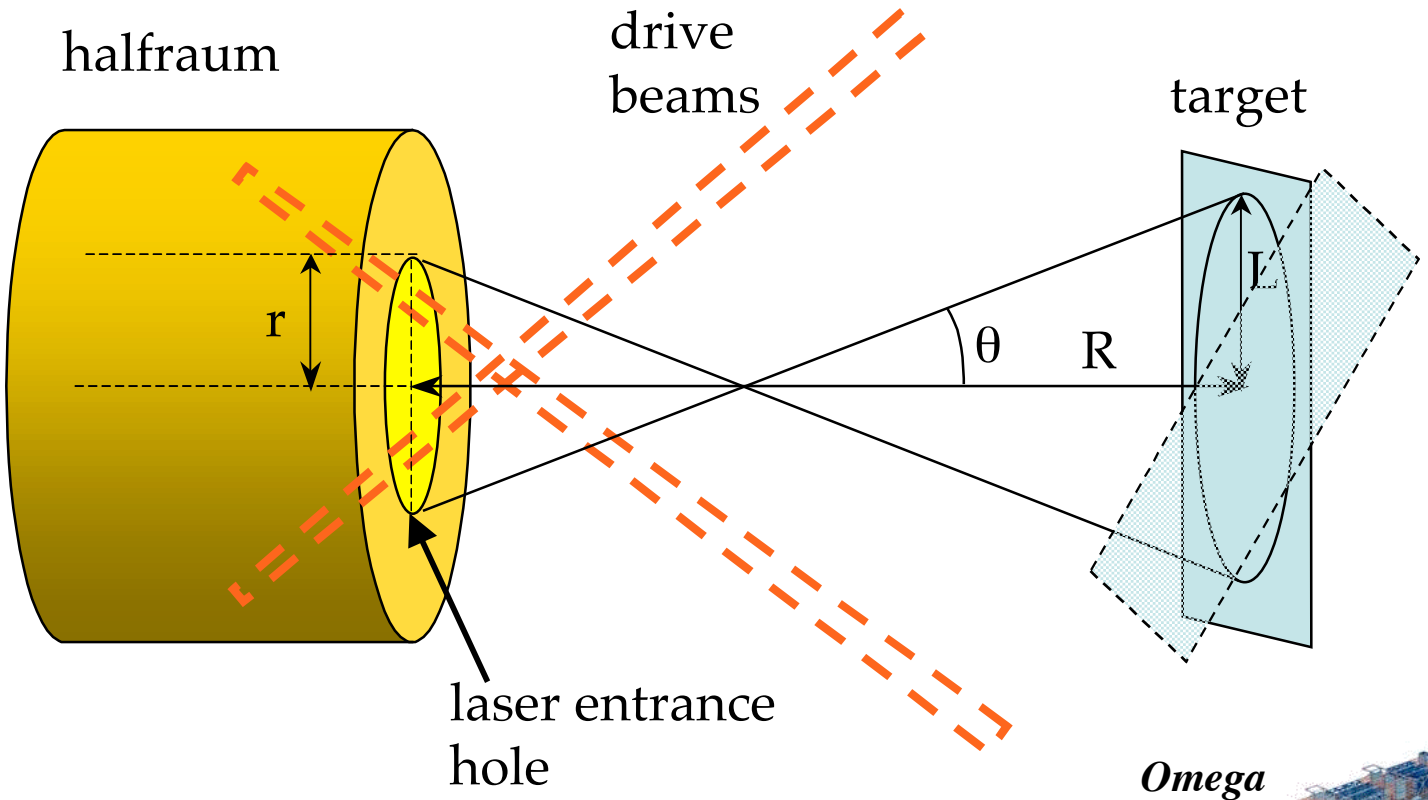

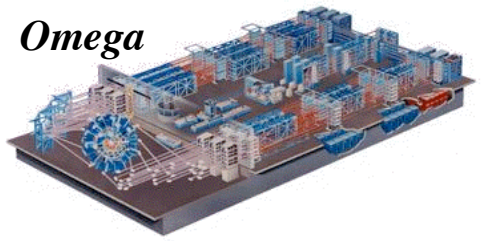

- By tilting the target we could also test the Tilted Radiation instability model